PHYSIOLOGICAL REVIEWS
Vol. 80, No. 2, April 2000
Printed in U.S.A.

Carbon Dioxide Transport and Carbonic Anhydrase in Blood and Muscle

CORNELIA GEERS AND GEROLF GROS

Zentrum Physiologie, Medizinische Hochschule, Hannover, Germany

Geers, Cornelia, and Gerolf Gros. Carbon Dioxide Transport and Carbonic Anhydrase in Blood and Muscle. *Physiol. Rev.* 80: 681–715, 2000.—CO_2 produced within skeletal muscle has to leave the body finally via ventilation by the lung. To get there, CO_2 diffuses from the intracellular space into the convective transport medium blood with the two compartments, plasma and erythrocytes. Within the body, CO_2 is transported in three different forms: physically dissolved, as HCO_3^-, or as carbamate. The relative contribution of these three forms to overall transport is changing along this elimination pathway. Thus the kinetics of the interchange have to be considered. Carbonic anhydrase accelerates the hydration/dehydration reaction between CO_2, HCO_3^-, and H^+. In skeletal muscle, various isozymes of carbonic anhydrase are localized within erythocytes but are also bound to the capillary wall, thus accessible to plasma; bound to the sarcolemma, thus producing catalytic activity within the interstitial space; and associated with the sarcoplasmic reticulum. In some fiber types, carbonic anhydrase is also present in the sarcoplasm. In exercising skeletal muscle, lactic acid contributes huge amounts of H^+ and by these affects the relative contribution of the three forms of CO_2. With a theoretical model, the complex interdependence of reactions and transport processes involved in CO_2 exchange was analyzed.

I. INTRODUCTION

One of the major requirements of the body is to eliminate CO_2. The large, but highly variable, amount of CO_2 that is produced within muscle cells has to leave the body finally via ventilation of the alveolar space. To get there, diffusion of CO_2 has to occur from the intracellular space of muscles into the convective transport medium blood, and diffusion out of the blood has to take place into the lung gas space across the alveolocapillary barrier.

Carbon dioxide in the body is present in three different forms: dissolved, bound as bicarbonate, or bound as carbamate. The relative contribution of these different forms to overall CO_2 transport changes markedly along this elimination pathway, because for diffusion across membrane barriers, another form is more appropriate than for transport within intra- or extracellular compartments. Thus the kinet-

ics of the interchange between forms become critically important. In addition, the products of one such interchange, the hydration reaction of CO_2, HCO_3^-, and H^+, are required for a great variety of other cellular functions such as secretion of acid or base and some reactions of intermediary metabolism. In exercising skeletal muscle, the other "end product" of metabolism, lactic acid, contributes huge amounts of H^+ and by these affects the predominance of the three forms of CO_2, because HCO_3^- as well as carbamate are critically dependent on the concentration of H^+. Discussion of the overall transport of CO_2 in skeletal muscle has to take into account this contribution of lactic acid and its involvement in kinetics and equilibria of CO_2 reactions. This interdependence of CO_2 and lactic acid elimination is one major aspect of this review, which as far as we know has not before been reviewed in detail.

II. CARBON DIOXIDE TRANSPORT IN BLOOD

A. Transport Forms of CO_2 in Blood

Carbon dioxide transport forms in blood have been thoroughly reviewed by Klocke (105). We only briefly summarize their respective contribution to overall CO_2 exchange. Table 1 sums up the contribution of the various forms in the two compartments plasma and erythrocytes: in whole arterial and venous blood during rest and during heavy exercise.

1. Dissolved CO_2

Only a small portion, ~5% of total arterial content, is present in the form of dissolved CO_2. Using a solubility coefficient S_{CO_2} of 3.21×10^{-5} M/Torr (35) for plasma at 37°C, this gives 1.28 mM dissolved CO_2, or, using S_{CO_2} of 3.08×10^{-5} M/Torr (7), 1.23 mM dissolved CO_2 at a P_{CO_2} of 5.32 kPa (40 Torr). At rest, the contribution of dissolved CO_2 to the total arteriovenous CO_2 concentration difference is only ~10%. However, during heavy exercise, the contribution of dissolved CO_2 can increase sevenfold and then makes up almost one-third of the total CO_2 exchange.

2. CO_2 bound as HCO_3^-

The majority of CO_2 in all compartments is bound as HCO_3^-. The ratio of HCO_3^- over dissolved CO_2 is given by the Henderson-Hasselbalch equation

TABLE 1. *CO_2 transport in blood at rest and exercise*

	Rest					Exercise		
	Arterial		Venous			Venous		
	mM	mmol/l blood	mM	mmol/l blood	v-a diff, mmol/l blood	mM	mmol/l blood	v-a diff, mmol/l blood
				Plasma				
pH†	7.40		7.37			7.145*		
P_{CO_2}	40		46			78*		
Dissolved	1.23	0.68	1.42	0.78	0.10	2.40	1.32	0.64
Bicarbonate	24.58	13.52	26.38	14.51	0.99	26.65*	14.66	1.14
Carbamate	0.54	0.30	0.55	0.30	0.01	0.44	0.24	−0.06
Sum plasma	26.35	14.49	28.35	15.59	1.10	29.49	16.22	1.72
				Red blood cell				
pH†	7.20		7.175			6.996		
Hb, g/l	333							
Hct†	0.45							
Hb_{O_2}, fract†	0.97		0.75			0.25		
Dissolved	1.23	0.4	1.42	0.46	0.06	2.40	0.78	0.38
Bicarbonate	15.47	5.01	16.84	5.46	0.44	18.91	6.13	1.11
Carbamate	1.66	0.75	1.86	0.84	0.09	2.12	0.95	0.21
Sum RBC	18.37	6.16	20.12	6.75	0.59	23.43	7.86	1.70
Total CO_2		20.65		22.34	1.69		24.08	3.42

Concentrations of the 3 forms of CO_2 in plasma and red blood cells (RBC) and their contribution to the concentrations in whole blood. Values of pH, P_{CO_2}, hemoglobin (Hb), hematocrit (Hct), and fraction of O_2-saturated hemoglobin represent assumed standard values. Blood gas values for venous plasma during heavy exercise (*) were taken from Bangsbo et al. (6). Dissolved CO_2 was calculated using a solubility coefficient, S_{CO_2} 0.0308 mM/Torr. Bicarbonate was calculated using −log of the dissociation constant of $pK'_a = 6.10$. Water content of erythrocytes was assumed to be 0.72, and extracellular pH (pH_o) was calculated from $pH_o = 0.796 \times (pH_{plasma} + 1.644)$ as given by Hilpert et al. (85). Carbamate concentrations in plasma were calculated using the equilibrium constants given by Gros et al. (61). For the calculation of carbamate concentrations in erythrocytes, the equilibrium constants pK_c, pK_z, and n from Gros et al. (68) were used with the exception of pK_c (β-chain deoxy), which was calculated from λ of Perella et al. (135) and pK_z (β-chain deoxy) of Gros et al. (68) to take into account the influence of 2,3-diphosphoglycerate concentration (see text). Units of mmol/l blood indicate contribution of the plasma and RBC, respectively, to the concentrations of each species to the concentration in whole blood. † Dimensionless quantities. v-a diff, arteriovenous difference.

$$pH = pK'_a + \log \frac{[HCO_3^-]}{S_{CO_2} \times P_{CO_2}}$$

The pK'_a has a normal value of 6.10 in human plasma at 37°C and varies with temperature and ionic strength (142). It appears to be slightly different in serum and red blood cells: serum, 6.11; oxygenated erythrocytes, 6.10; deoxygenated erythrocytes, 6.12 (8). During a heavy work load of the muscle, high levels of lactic acid are present in addition to CO_2, aggravating the decrease in pH. With this low pH, the fraction of HCO_3^- in total CO_2 is diminished. Although at pH 7.4 HCO_3^- is 20-fold compared with dissolved CO_2, it is only 13-fold at the normal intraerythrocytic pH of 7.2, and the ratio may fall to much lower values at plasma pH values of considerably below 7 during maximal exercise. Therefore, although the absolute arteriovenous difference is higher during exercise than during rest, the relative contribution of HCO_3^- to overall exchange is less. For the example of heavy exercise given in Table 1, HCO_3^- contributes only two-thirds of total CO_2 exchange, whereas at rest this figure is ~85%.

3. CO_2 bound as carbamate

The amount of CO_2 bound as carbamate to hemoglobin in erythrocytes or to plasma proteins depends on O_2 saturation of hemoglobin and 2,3-diphosphoglycerate (2,3-DPG) concentration in the case of erythrocytes, and on H^+ concentration in the case of both red blood cells and plasma (61, 68, 134, 135). During passage of blood through muscle, O_2 saturation and H^+ concentration change considerably, in particular during exercise. However, the increase in hemoglobin desaturation and the increase in H^+ concentration experienced by red blood cells in the capillary during exercise affect the amount of CO_2 bound to hemoglobin in opposite directions. Whereas deoxygenation of hemoglobin increases the amount of CO_2 bound to hemoglobin, acidification decreases the amount of carbamate formed by hemoglobin.

To calculate carbamate concentrations within erythrocytes, we use a single set of constants for the α- and β-chains in the oxy state of hemoglobin and separate constants for the α- and β-chains in the deoxy state. Because the calculation of carbamate is dependent on the values of the carbamate equilibrium constant (pK_c) and the ionization equilibrium constant of the amino group (pK_z) employed, errors in the determination of these constants in different studies can lead to changes in the calculation of the carbamate. Therefore, we use two different sets of constants to give an estimate of the variability of the calculated carbamate concentrations.

For oxyhemoglobin, we use the binding constants of Gros et al. (68) (number of CO_2 binding sites per hemoglobin tetramer $n = 2$, $pK_c = 4.73$, $pK_z = 7.16$), and for deoxyhemoglobin, their constants for the α-chain α-amino groups of $n = 2$, $pK_c = 5.19$, $pK_z = 7.05$. However, because their measurements were done in the absence of 2,3-DPG, their carbamate equilibrium constant (K_c) for the α-amino groups of the β-chains of deoxyhemoglobin was not used. On the other hand, intraerythrocytic concentration of 2,3-DPG has effectively no influence on the binding of CO_2 to oxyhemoglobin and to the α-chain α-amino groups of deoxyhemoglobin (132). For the β-chain α-amino group of deoxyhemoglobin, the ionization constant (K_z; $pK_z = 6.13$) estimated by Gros et al. (68) was used in conjunction with the CO_2 binding constant λ for this same amino group given by Perella et al. (135) for the presence of 2,3-DPG. Perella et al. (135) determined this figure by measuring CO_2 binding of hemoglobin whose α-amino groups were differentially blocked by cyanate. Using their value of λ, one obtains together with the above value of pK_z a carbamate equilibrium constant $pK_c = 5.06$ for these groups. Thus we describe CO_2 binding by the α-amino groups of the β-chains of deoxyhemoglobin in the presence of 2,3-DPG with $n = 2$, $pK_z = 6.13$, and $pK_c = 5.06$. With these constants we estimate a contribution of only ~5% (0.09 mM) of carbamate to overall CO_2 exchange during rest (Table 1). When the pK_z and pK_c values reported by Perella et al. (134) and the data of Perella et al. (135) are combined in an analogous fashion to estimate binding constants in the presence of 2,3-DPG, a contribution of 9% (0.16 mM) of carbamate to CO_2 exchange during rest is calculated. The former estimate of 0.09 mM or 5% agrees nicely with measurements of Böning et al. (13). From their data, an arteriovenous difference for carbamate of 0.09 mM is calculated for the blood gas values of Table 1. It should be noted that all these estimates of the contribution of carbamate to overall CO_2 exchange are lower than the value of 12.6% calculated by Klocke (105). However, Klocke's use of the data of Perella et al. (135), which are valid for pH 7.4 rather than the normal intraerythrocytic pH 7.2, may have led to a substantial overestimate of the role of carbamate because carbamate formation increases drastically with increasing pH. Thus it appears that a contribution of 5% by carbamate is a reasonable estimate although markedly lower than previously believed.

During heavy exercise as defined in Table 1, ~6% (10.8% with the data of Perella and co-workers, Refs. 134, 135) of the arteriovenous concentration difference of total CO_2 is calculated to be due to a change in carbamate. Böning et al. (13) have measured an ~10% contribution to overall exchange during aerobic exercise, but during heavy exercise with considerable anaerobic metabolism they found that carbamate does not contribute to CO_2 exchange at all; arterial blood contained a carbamate concentration that was higher by 0.06–0.13 mol/mol hemoglobin than that of venous blood in the presence of lactic acid. The data of Table 1 thus represent an inter-

mediate position between these extreme types of exercise.

Carbamate concentration in plasma does not contribute to overall CO_2 exchange according to Table 1, which is in agreement with Klocke's conclusion (105). During heavy exercise, arterial plasma contains an even higher concentration of carbamate than venous plasma. The physicochemical reason for this is that, in the absence of an oxylabile carbamate fraction as exhibited by hemoglobin, the increase in carbamate by the elevated P_{CO_2} in venous plasma is counteracted or overruled by a decrease in carbamate caused by the fall in pH.

B. Transport Within the Intracellular Compartment

Figure 1 shows that overall CO_2 transport is the sum of the diffusion of *1)* dissolved CO_2 and *2*) CO_2 bound as HCO_3^-. The contribution of HCO_3^- to CO_2 transport is called "facilitated CO_2 diffusion" and was first described by Longmuir et al. (111). Gros and Moll (66) and Gros et al. (67) have shown that facilitated CO_2 diffusion involves a flux of H^+ equivalent to that of HCO_3^-, a fact which matches the other fact that hydration of CO_2 produces equal amounts of H^+ and HCO_3^-. Facilitated CO_2 diffusion by HCO_3^- diffusion under steady-state conditions then requires *1*) rapid conversion of CO_2 into HCO_3^- and H^+, which at the short diffusion distances as they occur in cells (<1 mm) implies that the presence of carbonic anhydrase (CA) catalyzing CO_2 hydration is essential for facilitation to occur, and *2*) equal fluxes of H^+ and HCO_3^-, where *3*) significant fluxes of H^+ can only be achieved when they occur by facilitated H^+ diffusion, i.e., by the diffusion of mobile buffers carrying H^+ and present at concentrations comparable to that of HCO_3^-. This leads to the following scheme of facilitated CO_2 diffusion shown in Figure 1.

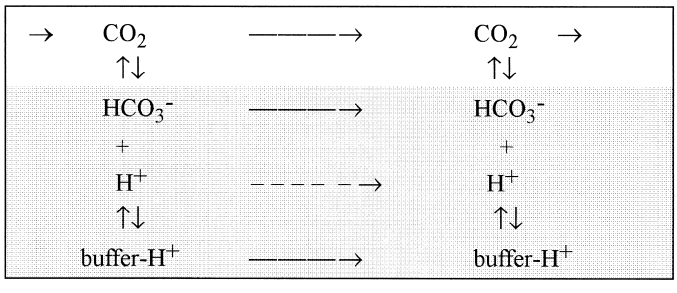

FIG. 1. Mechanism of facilitated diffusion of CO_2. White background area indicates free diffusion (physically dissolved) CO_2, and the shaded background indicates the process of facilitated CO_2 diffusion. "Buffer" is any mobile buffer with an appropriate p*K* value, such as phosphate at pH ~7.

TABLE 2. *Diffusion coefficient of dissolved CO_2 in water and hemoglobin solutions*

Medium	Temperature, °C	Diffusion Coefficient, cm^2/s	References
Water	22	1.71×10^{-5}	Gros and Moll (64)
	38	2.5×10^{-5}	Gros and Moll (64)
16 g% Hemoglobin	38	1.6×10^{-5}	Gros and Moll (64)
33 g% Hemoglobin	38	1.14×10^{-5}	Gros and Moll (64)
100% Hemolysate (33 g%)	37	0.34×10^{-5}	Uchida et al. (173)

1. Diffusion of dissolved CO_2

Diffusion coefficients (=diffusion constant/S_{CO_2}) have been measured under conditions where only little facilitated diffusion is present. In a 33g% hemoglobin solution, the hemoglobin concentration that prevails inside the red blood cell, the CO_2 diffusion coefficient, is reduced to less than one-half of its value in water (Table 2). It is not clear why the figure of Uchida et al. (173) is three times lower than the figure of Gros and Moll (64) for this condition. Compared with diffusion in water, diffusion is hindered by the presence of hemoglobin as it is by the presence of other intracellular proteins. It appears that proteins are virtually impermeable to CO_2 and represent the major obstacles to CO_2 diffusion within cells (64). Accordingly, CO_2 diffusion constants decrease in a defined manner with increasing hemoglobin concentration (curve in Fig. 2) that can be explained quantitatively on the basis of the geometry of the water space in a hemoglobin solution (64). Similarly, the CO_2 diffusion constant in various tissues varies systematically with the protein concentration of these tissues (points in Fig. 2). It is obvious that, for a given protein concentration, the CO_2 diffusion constants in these different cells or tissues agree very nicely.

2. Diffusion of HCO_3^-

The diffusion coefficients for HCO_3^- are about one-half as great as those for CO_2, and in the presence of proteins, its diffusion can be expected to be hindered to an extent comparable to that observed for CO_2 diffusion. The HCO_3^- diffusion coefficient is calculated from the equivalent conductivity of HCO_3^- (67, 108), 11.7×10^{-6} cm^2/s in pure water at 25°C, and is reduced to 8.7×10^{-6} cm^2/s at physiological ionic strength and 25°C (67). Again, Uchida et al. (173) report a surprisingly low value of 1.4×10^{-6} cm^2/s for HCO_3^- diffusion in "100% hemolysate" at 37°C. The relative contribution of HCO_3^- to total CO_2 diffusion (=facilitated diffusion) can be evaluated on the basis of these diffusion coefficients. The contribution of HCO_3^- diffusion, and thus of facilitated diffusion, to total CO_2 diffusion depends greatly on the partial pressure

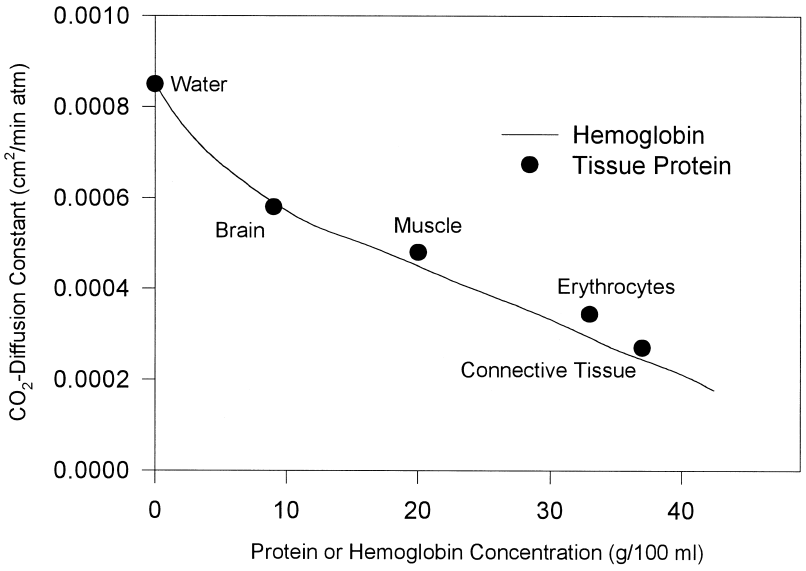

FIG. 2. Diffusion constants of CO_2 (in $cm^2 \cdot min^{-1} \cdot atm^{-1}$) at 22°C in different tissues as a function of the protein concentration (points) and in hemoglobin solutions of different hemoglobin concentrations (solid line). [Redrawn from Gros and Moll (64).]

range of CO_2 in which the transport process takes place. This can be predicted from the general shape of CO_2 binding curves, which are steep at low P_{CO_2} values and become flatter with increasing P_{CO_2}. Therefore, the HCO_3^- concentration gradient per CO_2 concentration gradient is higher at low P_{CO_2}, and vice versa. This implies that the relative contribution of facilitated diffusion is highest at lowest P_{CO_2} values and decreases consistently with increasing P_{CO_2} (66, 67).

3. Diffusion of H^+

The diffusion coefficient of free H^+ in aqueous solutions at 25°C is 9.3×10^{-5} cm^2/s (123), i.e., H^+ possess a more than five times greater diffusivity in water than CO_2. Nevertheless, free diffusion of H^+ is a rather ineffective mechanism of H^+ transport, because at physiological values of pH, the H^+ concentration gradients within cells cannot exceed the order of 10^{-7} to 10^{-8} M. In the presence of buffering substances at physiological concentrations of 10^{-3} to 10^{-2} M, such differences of free H^+ concentrations are accompanied by concentration differences of buffered H^+ of at least of 10^{-3} to 10^{-2} M or more. This very much higher concentration difference of the bound H^+ compensates for the lower diffusion coefficients of mobile buffers. The diffusion coefficient for a mobile buffer such as phosphate is of the same order of magnitude as that of HCO_3^-, 7.0×10^{-6} cm^2/s (67). Consider as an example an intracellular pH difference of 0.1 between absolute pH values of 7.1 and 7.2; then, the expected flux of H^+ by free H^+ diffusion, estimated as diffusion coefficient (D) × concentration difference (Δc), gives $9.3 \times 10^{-5} \times 1.62 \times 10^{-8}$ $mmol \cdot cm^{-1} \cdot s^{-1} = 1.5 \times 10^{-12}$ $mmol \cdot cm^{-1} \cdot s^{-1}$. Estimating facilitated H^+ flux by diffusion of buffered H^+ with the assumption of a buffer capacity of 40 mM/ΔpH and the above value of D for phosphate in an analogous fashion yields $7.0 \times 10^{-6} \times 0.1 \times 40 \times 10^{-3}$ $mmol \cdot cm^{-1} \cdot s^{-1} = 2.8 \times 10^{-8}$ $mmol \cdot cm^{-1} \cdot s^{-1}$. Thus facilitated H^+ diffusion by buffer diffusion in this example is more than 10,000 times more effective than free diffusion of H^+. It has been shown that not only the diffusion of low-molecular-weight buffers such as phosphate (67) but also the diffusion of protein buffers (66) is a highly effective means of H^+ transport. In the case of very large protein molecules, it has even been shown that facilitated H^+ transport occurs very efficiently not only by translational but in addition by rotational protein diffusion (62, 63). Thus facilitated CO_2 diffusion essentially occurs by diffusion of HCO_3^- and simultaneous buffer-facilitated H^+ diffusion. That buffer mobility is indispensable for this process to take place has been shown by Gros et al. (67) by demonstrating that immobilized phosphate buffer cannot entertain facilitated CO_2 diffusion.

Al-Baldawi and Abercrombie (3) have reported measurements of H^+ diffusion in cytoplasm extracted from giant neurons of a marine invertebrate. An apparent diffusion coefficient for H^+ of only 1.4×10^{-6} cm^2/s was determined, which was 5 times lower than the estimated diffusion coefficient of the mobile buffers and 70 times lower than the diffusion coefficient of free H^+. This appears to be in contradiction to the above considerations. However, because the authors performed their measurements under non-steady-state conditions by observing the relaxation of pH after a sudden pH change at one surface of the cytoplasm sample, it appears likely that this value represents a substantial underestimate of the apparent H^+ diffusivity that one would observe under steady-state conditions. A pH transient will be greatly slowed down by

the presence of buffers whose buffering capacity is so overwhelming compared with free H^+ concentration. This problem was aggravated in the experiments of Al-Baldawi and Abercrombie (3) by the presence in the cytoplasm of a substantial fraction of immobile buffers.

The contribution of facilitated diffusion to overall diffusion depends on the actual concentration differences for HCO_3^- and for buffered H^+. These in turn are dependent on the actual pH gradient and the p*K* value(s) of the mobile buffer(s) present. As an example, calculated CO_2 fluxes are shown in Figure 3 as a function of the average pH with boundary P_{CO_2} values of 5.32 and 6.65 kPa (40 and 50 mmHg) in a 66 mM phosphate solution (p*K* 6.84, 25°C). Total CO_2 diffusion is more than twice as high as free diffusion of dissolved CO_2 in a pH range of ~6.9–7.8. Thus more than one-half of the CO_2 transport in this model system occurs by facilitated diffusion, which means that at a physiological pH of the intracellular or extracellular spaces more HCO_3^- than CO_2 molecules contribute to total CO_2 flux within the compartment. Facilitated diffusion does not reach its maximum exactly at the p*K* value of the phosphate, i.e., at the maximal buffer capacity of the solution. The reason for this is that whereas above pH 6.84 the buffer capacity decreases, the pH difference across the layer increases markedly. The sum of these two effects leads to an increase with increasing pH in the concentration differences of HCO_3^- and of the H^+-carrying $H_2PO_4^-$ beyond the p*K* of the phosphate buffer. Under physiological conditions, the course of this curve may be different, since buffering is accomplished by different sets of buffers with more than one p*K* value. Although proteins, which are important buffers in intact cells, possess a lower diffusivity than inorganic phosphate, their large buffer capacity for H^+ results in a facilitation of CO_2 diffusion in intact cells that is of a similar order of magnitude as shown in Figure 3 for phosphate. For the condition within red blood cells, in a hemoglobin solution of 30 g% Hb at 38°C and at roughly physiological pH and P_{CO_2}, Gros and Moll (65) have measured a contribution of facilitated CO_2 diffusion of ~85% to total intraerythrocytic CO_2 transport.

C. Transport Across the Erythrocyte Membrane

Although total CO_2 flux across the membrane can again be considered as the sum of diffusion of dissolved CO_2 and of HCO_3^- with accompanying H^+, the relative contributions of dissolved and bound CO_2 to overall CO_2 flux across the erythrocyte membrane are quite different compared with diffusion within the intracellular compartment.

1. Dissolved CO_2

Cell membranes are generally considered to be highly permeable to gases such as CO_2 or O_2, with one of the few exceptions being the apical membrane of parietal and chief cells of gastric glands, which have been described to possess "no detectable permeability to NH_3, NH_4^+, CO_2, and HCO_3^-" and whose surface area times permeability product was found to be about three orders of magnitude lower than that of the basolateral membranes of the same cells (15, 176). Erythrocyte membranes, though, are highly permeable to CO_2, the absolute permeability values cited being in the range of 0.35–3 cm/s (Table 3), as has been thoroughly discussed by Klocke (105). More recently, Forster et al. (47) measured the rate of depletion of $C^{16}O^{18}O$ in erythrocyte suspensions by mass spectroscopy. They evaluated their measurements

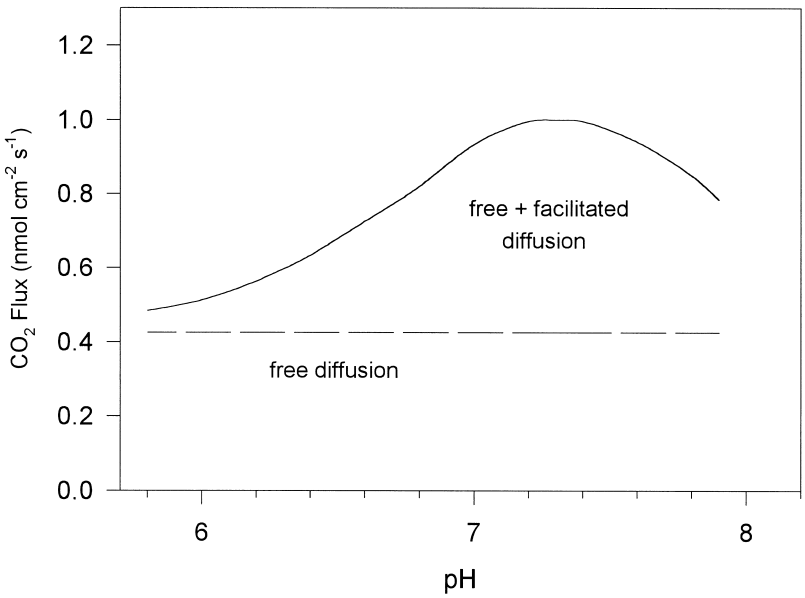

FIG. 3. Calculated CO_2 fluxes across a layer of buffer solution as a function of the average pH value in this layer. The boundary CO_2 partial pressures are constant with 6.65 and 5.32 kPa (50 and 40 mmHg), respectively. The solution is 66 mM phosphate with varying contents of base. Thickness of the layer is 180 μm. Carbonic anhydrase is assumed to be present in excess. Solid curve represents the total flux of CO_2, and dashed curve represents the flux by free diffusion only. [Redrawn from Gros et al. (67).]

TABLE 3. *Permeability of erythrocytic and other membranes*

	Permeability, cm/s	References
CO_2		
Extrapolated, from NH_3 measurements, erythrocytic membrane	0.58	Forster (43)
Calculated from comparison of diffusion in hemoglobin solution vs. red cell suspension	>3.0	Gros and Moll (64)
Lipid bilayer	0.35	Gutknecht et al. (71)
Calculated from comparison of diffusion in hemoglobin solution vs. red cell suspension	1.6	Gros and Bartag (59)
Red blood cells, mass spectroscopy	~1	Forster et al. (47)
HCO_3^-		
Phospholipid vesicles, 25°C	4.3×10^{-6}	Norris and Powell (127)
Frog skeletal muscle, room temperature	2×10^{-7}	Woodbury and Miles (188)
Human erythrocytic membrane, 37°C	5.6×10^{-4}	Sieger et al. (160)
H^+/OH^-		
Phospholipid vesicles, 25°C	1.8×10^{-5}	Norris and Powell (127)
Erythrocytic membrane, at pH_o 7.4, 37°C	2.4×10^{-3}	Crandall et al. (22)

pH_o, extracellular pH.

to give the CO_2 permeability of the human red cell membrane and obtained a value of ~1 cm/s. If we simplistically equate physiological CO_2 concentration with CO_2 concentration difference across the membrane (c_{CO_2}), we can estimate the possible order of magnitude of physiologically occurring CO_2 fluxes from $P_{CO_2} \times c_{CO_2}$ = 1 cm/s × 1 mM = 1×10^{-3} mmol·cm^{-2}·s^{-1}.

2. HCO_3^-

Permeability for HCO_3^- of artificial phospholipid vesicles, which are devoid of any anion exchanger, is six orders of magnitude lower (Table 3; Ref. 127) than it is for dissolved CO_2. However, erythrocyte membranes of all vertebrates with the exception of agnathans (hagfishes and lampreys; see reviews, Refs. 80, 126, 136) do have a rapid anion (HCO_3^-/Cl^-) exchange protein, capnophorin or band 3 (see review by Jennings, Ref. 90), which exchanges HCO_3^- for Cl^- at a ratio of 1:1. An overview of the distribution of this transporter in red blood cells is given in Table 4. Thus the permeability of the erythrocyte membrane to HCO_3^- is considerably increased over that of lipid bilayers but still about three to four orders of magnitude lower than the permeability for dissolved CO_2 (Table 3). Net driving force for HCO_3^-/Cl^- exchange is proportional to the difference in the electrochemical potential for both ions. The turnover number of this transporter is 4–5 × 10^4 Cl^-·s^{-1}·transporter molecule^{-1} at 37°C (16, 56). With this figure and the number of 1.0–1.2 × 10^6 copies of capnophorin per red blood cell (90), a maximal flux across the membrane of ~6 × 10^{-5} mmol Cl^-·cm^{-2}·s^{-1} can be calculated using an erythrocytic volume of 80 × 10^{-12} cm^3 and a red cell surface of 1.6 × 10^{-6} cm^2. Maximal HCO_3^- flux is expected to be in the same range as that of Cl^-. Flux measurements at 0°C have shown a maximal value for HCO_3^- flux of 1% of this theoretical value, ~5 × 10^{-7} mmol HCO_3^-·cm^{-2}·s^{-1} (48). When the large temperature dependence of the anion transporter with a turnover number at 0°C of only ~200 Cl^-·s^{-1}·molecule^{-1} (56) is taken into account, this agrees well with the value calculated above for maximal flux at 37°C. Values of HCO_3^- permeability of erythrocyte membranes are similar for humans and birds (as well as in several other species). In red blood cells of adult humans and of chicken HCO_3^- permeability ($P_{HCO_3^-}$) was measured to be 5.6 × 10^{-4} and

TABLE 4. *Carbonic anhydrase activity and HCO_3^-/Cl^- exchanger in blood of different species*

	Plasma			Red Blood Cell		
	CA available to plasma	CA in plasma	CA plasma inhibitor	CA I	CA II	HCO_3^-/Cl^- exchanger
Mammals (human, dog, rat, rabbit, mouse)	+Lung[h] +Muscle[i]	−		+[a]	+[a]	+
Dog, pig, sheep, rabbit		−	+[b]	+	+	+
Ox, domestic cat, lion, jaguar, tiger, leopard		−		−[m]	+[m]	+
Birds (chicken)				−[c]	+	+
Amphibian (frog)				−[c]	+	+
Teleosts (trout, eel, flounder)	+Gill[n]		+[d]	+	+	+
Trout	+Muscle[j]		+			
Elasmobranchs (dogfish)	+Gill[l]	+[e]		+[c,o]	−	+[f]
Agnathans (hagfish, lamprey)	−Gill[k]			+[o]	−	−[g]

Carbonic anhydrase (CA) I and CA II, respectively, or isozymes are functionally similar to these mammalian isozymes. Data were taken from the following references: [a] 113; [b] 83, 109; [c] 115; [d] 74, 75, 136; [e] 186; [f] 129; [g] 39, 131, 171, 172; [h] review, 11; [i] 25, 37, 128, 175, 179, 189; [j] 82; [k] 79; [l] 167; [m] 18; [n] 28; [o] 114.

7×10^{-4} cm/s, respectively (160). These latter authors showed that a functionally active band 3 protein is present in the erythrocyte membrane of the chicken at very early stages of development. In the dogfish (*Mustelus canis*), flux of HCO_3^- across red cell membrane was reported to equal flux across human red cell membranes (128). It should be mentioned that a very large number of measurements have been reported for the HCO_3^- permeability of the human red blood cell (e.g., Refs. 19, 30, 88, 103), most of which yielded numbers very similar to that of Sieger et al. (160), as cited in Table 3. Estimating the physiologically possible HCO_3^- flux across the red cell membrane in a fashion analogous to that used above for CO_2, one obtains the following: $P_{HCO_3^-} \times c_{HCO_3^-} = 5 \times 10^{-4}$ cm/s $\times$ 10 mM $= 5 \times 10^{-6}$ mmol·cm^{-2}·s^{-1}, which is ~10 times less than the maximal flux of 6×10^{-5} mmol·cm^{-2}·s^{-1} estimated above from turnover number and number of copies of capnophorin per red blood cell but more than two orders of magnitude smaller than the above CO_2 flux.

3. H^+

Proton permeability of phospholipid vesicles is five times higher than HCO_3^- permeability, 1.8×10^{-5} cm/s (127). However, because the H^+ concentration gradient across the cell membrane is very small (intracellular pH 7.2, extracellular pH 7.4, ΔpH 0.2), the product permeability × concentration gradient, is also very small: $P_{H^+} \times c_{H^+} = 1.8 \times 10^{-5}$ cm/s $\times$ 2.3×10^{-8} M $= 4 \times 10^{-13}$ mmol H^+·cm^{-2}·s^{-1}. Thus diffusion of free H^+ across the membrane is so small that it cannot support any facilitated CO_2 diffusion. However, in addition to free H^+ diffusion, there are several other more efficient mechanisms of H^+ transport across the red cell membrane. The significance of these pathways for overall H^+ flux across the erythrocytic membrane depends on the specific conditions. Proton fluxes (or reverse OH^+ fluxes) in erythrocyte membranes can be achieved via *1*) the Jacobs-Stewart cycle, which includes HCO_3^-/Cl^- exchange via capnophorin; *2*) H^+ flux via HCl cotransport (or OH^+-Cl^- countertransport); and *3*) H^+ flux via H^+-lactate cotransport and nonionic lactic acid diffusion.

Bisognano et al. (12) measured H^+ fluxes across red cell membranes by a pH stat method. They induced these fluxes by establishing an outward Cl concentration gradient through increasing the osmotic strength of the extracellular solution with sucrose. Without lactate/lactic acid present, two-thirds of the measured apparent H^+ flux was mediated via the Jacobs-Stewart cycle (89), and one-third was due to a DIDS-sensitive HCl cotransport. The Jacobs-Stewart cycle brings about a H^+ efflux from the red blood cell by the following sequence of processes: *1*) H^+ in the cell reacts with HCO_3^- to give CO_2, *2*) CO_2 leaves the cell and *3*) is hydrated extracellularly to give H^+ and HCO_3^-, where *4*) the H^+ remains outside while the HCO_3^- enters the cell in exchange for Cl^- via the Cl^-/HCO_3^- exchanger. Bisognano et al. (12) base their study on the assumption that the Jacobs-Stewart cycle-mediated H^+ flux is inhibitable by the CA inhibitor ethoxzolamide, whereas HCl cotransport is not affected by this drug but suppressed by DIDS. Under their conditions, an initial flux via HCl cotransport was observed at 0.5×10^{-9} mmol H^+·cm^{-2}·s^{-1}, compared with 1×10^{-9} mmol H^+·cm^{-2}·s^{-1} mediated by the Jacobs-Stewart cycle, giving a total H^+ flux by these two mechanisms of 1.5×10^{-9} mmol·cm^{-2}·s^{-1}.

Compared with free H^+ diffusion, this value is very high; it is considerably lower than the HCO_3^- flux estimated above and substantially lower than the estimated CO_2 flux.

A third mechanism of H^+ transport across the red cell membrane is by the H^+/lactate carrier and by nonionic diffusion of lactic acid, both of which require the presence of lactate (27, 138). Proton fluxes via this mechanism were calculated from flux measurements of Fishbein et al. (42) and of Poole and Halestrap (138) in human red blood cells to be 2–2.5 $\times$ 10^{-9} mmol H^+·cm^{-2}·s^{-1}. Thus, in the presence of lactate, the above H^+ flux estimate would have to be raised to ~4×10^{-9} mmol·cm^{-2}·s^{-1}, which is much lower than the flux estimate for HCO_3^-. The fluxes of both ions, however, are more than two orders of magnitude smaller than a physiological CO_2 flux. Thus a significant facilitation of CO_2 diffusion across the red cell membrane does not occur. It may be noted that the activity of the H^+-lactate cotransport can be increased considerably in *Plasmodium falciparum*-infected human erythrocytes (96).

In conclusion, the permeability of dissolved CO_2 is much greater than the effective permeability of HCO_3^- and H^+. At the same time, more than two-thirds of the CO_2 transported in either red blood cells or plasma is transported in the form of HCO_3^-. This makes it appear essential that CO_2 and HCO_3^- can be converted into each other quite rapidly at the boundary between the two compartments: intraerythrocytic space and plasma. A high velocity of this interconversion is achieved by the enzyme CA.

Although HCO_3^- and H^+ are produced in equal amounts by the hydration of CO_2, the distribution of the two products among the two compartments, intraerythrocytic space and plasma, is quite different at electrochemical equilibrium. Bicarbonate is transported to a larger fraction within plasma than within erythrocytes because the equilibrium pH of the plasma is more alkaline than the intraerythrocytic pH (Table 1). In contrast, H^+ are transported to a larger fraction within erythrocytes than in plasma because the nonbicarbonate buffer capacity of erythrocytes exceeds that of plasma by a factor of ~10.

The CO_2 entering the blood during capillary passage through the peripheral tissue can encounter two different situations: *1*) a situation where CA is present in red blood

cells only, or *2*) a situation where CA is available in red blood cells and in plasma,

A) RAPID CATALYSIS OCCURS ONLY WITHIN ERYTHROCYTES. Carbon dioxide enters the red blood cells, and there is rapidly converted to HCO_3^- and H^+. When the red blood cell has reached the end of the capillary, electrochemical equilibrium across erythrocyte membrane is not yet established, because H^+ concentration and even more so HCO_3^- concentration are too high within red blood cells compared with plasma concentrations. A significant fraction of the intraerythrocytic HCO_3^- has left the cell via HCO_3^-/Cl^- exchange already during capillary transit. After blood has left the capillary, part of HCO_3^- and H^+ that has been produced within the red blood cell is dehydrated back to give CO_2; CO_2 then leaves the cell and enters the plasma, where the slow uncatalyzed reaction hydrates CO_2 to establish final equilibrium. During this postcapillary process, the plasma pH shifts slowly in the acidic direction.

B) RAPID CATALYSIS OCCURS IN ERYTHROCYTES AND IN PLASMA. Carbon dioxide enters red blood cells and is rapidly converted there, but also within plasma, to HCO_3^- and H^+. Equilibration between the two compartments is no longer rate limited by the slow CO_2 hydration reaction in plasma. The pH of the blood leaving the capillary can be expected to be constant and in equilibrium. However, as is shown in section IV*D2*, in the presence of lactic acid production in the tissue, this must not necessarily be so. At the end of capillary transit, it may even be possible that H^+ concentration in plasma is too high compared with intraerythrocytic concentration for equilibrium to be established across the erythrocytic wall, since equilibration of lactic acid across this wall is a slow process.

For CO_2 excretion, it is essential that there is a rapid chemical reaction of CO_2. However, how and how fast acid-base equilibrium is established in the blood depends on the sites of CA localization and its activity. This and the velocity of other CO_2 reactions will therefore be considered in the following sections.

E. Interconversion Between CO_2 and HCO_3^-

The interconversion between CO_2 and HCO_3^- without a catalyst is rather slow and may require more than 1 min to approach completion, a time much too long compared with the capillary transit time, which is ~1 s. Carbon dioxide hydration/dehydration reactions are accelerated between 13- and 25,000-fold by intraerythrocytic CA activities (46, 47). With such a CA activity, the interconversion between CO_2 and HCO_3^- inside erythrocytes requires only 2 ms for 95% completion.

The participants of this reaction, HCO_3^- and, in particular, the H^+ (see sects. III*C1*, III*D*, and IV) are involved in other reactions, so the time course of their concentration is also dependent on the kinetics of other reactions. For a complete understanding of the overall time course of CO_2 exchange, these reactions have also to be considered.

1. Catalysis by CA in blood

Carbonic anhydrase is found in the blood of all vertebrates. With respect to location, isozyme types, and coexpression of the anion exchanger (capnophorin), there are very interesting variations between different species from the lower vertebrates to mammals (Table 4) that may shed light on the increasing efficiency of CO_2 excretion in the course of evolution.

A) CYTOPLASM OF ERYTHROCYTES. Carbonic anhydrase was first detected by Meldrum and Roughton (118) [for review, see Maren (113) and Klocke (105)]. Briefly, isozyme CA I with a relatively low specific activity occurs in the red blood cells of all vertebrate groups with the exception of the cat family and a few other species; it is absent in the red blood cells of the cat, lion, jaguar, tiger, leopard, ox, chicken, and frog (18, 115). In primitive agnathans (lamprey, hagfish) and elasmobranchs (dogfish), CA I is the only isozyme present (114). It is somewhat less inhibitable by sulfonamides and considerably more susceptible to anions than CA II. Isozyme CA II with a specific activity that is ~10 times higher than that of CA I is probably the most widespread form and occurs in the red blood cells of all vertebrates except agnathans and elasmobranchs.

A mechanism for rapid HCO_3^-/Cl^- exchange across the erythrocyte membrane is present in almost all vertebrate red blood cells and is missing only in the most primitive vertebrate group, the agnathans (lamprey, hagfish; Refs. 39, 131, 171, 172). The consequence of this has been discussed by Nikinmaa (126). In these fish this precludes the utilization of plasma HCO_3^- in CO_2 excretion on a physiological time scale. Together with the rather flat CO_2 binding curve, CO_2 transport in these animals appears rather inefficient, yet in the lamprey, CO_2 transport potential is as great as in the highly active teleosts despite the missing anion exchanger. In this species, the disadvantage is overcome by a high intraerythrocytic pH, resulting in a high intracellular binding capacity for CO_2 and a marked Haldane effect. However, the intracellular buffering capacity is separated from the plasma compartment in lampreys due to the low membrane permeability to HCO_3^-. As a consequence, extracellular metabolic acid loads cause marked fluctuations in plasma pH. Thus the major advantage gained by the rapid anion exchanger appears to consist of an improved effective extracellular buffering (with access to the intracellular buffering power) rather than in a major improvement of gas transport (126).

The acceleration of the hydration-dehydration velocity by CA within erythrocytes is considerable. An activity (factor by which the rate of CO_2 hydration is accelerated) of 13–14,000 was reported by Forster and Itada (46), and

figures of 23,000 and 25,000 have been obtained by Wistrand (184) and by Forster et al. (47). The cytosolic CA enzymes may be not uniformly distributed within the red blood cells. Some indications have been proposed to suggest that their concentration may be increased near the cellular border. Interactions of CA are reported with the plasmalemmal anion exchanger (capnophorin = band 3; Ref. 98), and it would seem a most efficient place to catalyze CO_2-HCO_3^- hydration-dehydration reaction in close neighborhood to HCO_3^-/Cl^- exchange. Parkes and Coleman (133) reported an enhancement of CA activity by erythrocytic membranes; CA II and CA I activity were increased 3.5- and 1.6-fold, respectively, by the presence of red cell membranes. Whether in their erythrocytic membrane preparation the effective structure was the band 3 protein can only be speculated. Although these observations have not been confirmed yet by other investigators, there are several studies of the problem whether part of red cell CA is firmly bound to the erythrocyte membrane. Whereas Enns (40) had found CA in red cell ghosts, later studies by Tappan (170), Rosenberg and Guidotti (145), and Randall and Maren (139) came to the conclusion that red cell CA is a truly cytosolic enzyme and not membrane bound.

B) PLASMA. No CA activity aside from that attributable to lysed erythrocytes was ever found in plasma, with the sole exception of dogfish (*Scyliorhinus canicula*; Ref. 186). Also, there is no CA activity on the outside surface of erythrocytes or available to plasma, as was confirmed by Effros et al. (37).

However, in tissues where especially large amounts of CO_2 leave or enter the blood, there is extracellular catalysis available to the capillary plasma in some species. This is achieved by an extracellular CA bound to membranes, the membrane-bound isozyme CA IV, which provides catalytic activity to the plasma. Such a membrane-bound CA was found in the lung (36, 104, 150) and gill (28). In skeletal muscle, the first evidence for the presence of such a CA in dog, cat, and rabbit was provided by measurements of the distribution space of labeled HCO_3^- (37, 50, 51, 189) and by measurements of the postcapillary pH kinetics (128).

With the histochemical method of Hanson, staining of endothelial membranes as well as sarcolemma was observed in skeletal muscle (140, 141). Immunohistochemical studies employing anti-CA IV antibodies at the light microscopic level revealed staining of capillary walls, which would indicate that CA IV is associated with endothelial cell membranes (157). With the use of semithin sections and a more sensitive immunocytochemical technique, however, capillaries and sarcolemma were found to be stained, and in antibody-treated ultrathin sections of skeletal muscle studied by electron microscopy, membrane-bound CA IV was found to be associated with capillary endothelium, sarcolemma, and sarcoplasmic reticulum (SR) (24). That sarcolemmal and SR CA IV were visible in ultrathin sections but not in cryosections was attributed to a poor accessibility of CA IV at these locations in the 7-μm-thick untreated cryosections. Another approach has been used by Geers et al. (51). Measuring the space of distribution of labeled HCO_3^- and its reduction by CA inhibitors, Geers et al. (51) observed that the effectiveness of macromolecular CA inhibitors of different molecular size (Prontosil-dextrans of mol wt 5,000 vs. 100,000) indicates the presence of CA in the interstitial space. Indirect although strong evidence for this CA to be associated with the sarcolemma was obtained by intracellular and cell surface pH microelectrode measurements on skeletal muscle fibers by deHemptinne et al. (25). They observed a transient alkaline pH shift on the surface of these fibers upon exposure to propionate, whose magnitude was greatly increased in the presence of the CA inhibitor acetazolamide in the extracellular space. This was interpreted to show that in the presence of extracellular sarcolemmal CA CO_2-HCO_3^- acts as a rapid and efficient source of H^+ that enter the cells together with the propionate ion. Analysis of isolated sarcolemmal vesicles demonstrated the presence of high activities of CA associated with the sarcolemma (179), and it was shown by Western blotting with anti-CA IV antibody that this sarcolemmal CA is isozyme CA IV (175). In conclusion then, the present state of evidence indicates that in skeletal muscle, membrane-bound CA IV is associated with endothelial as well as with sarcolemmal membranes, in addition to a CA bound to the sarcoplasmic reticulum membrane.

In the case of lung tissue, it was estimated by Bidani et al. (11) that the CA of rat pulmonary vasculature catalyzes the extracellular hydration-dehydration reaction by a factor of 130–150, a figure that may appear rather small compared with the intraerythrocytic activity of >10,000. However, the calculations described below indicate that an activity of 100 in the plasma within the capillary bed of skeletal muscle should be sufficient physiologically (see sect. IV*D2*). No estimates of intracapillary CA activity in muscle capillaries are available.

The localization pattern of CA in blood is further complicated by the presence of a CA inhibitor in the plasma of some species, which ensures the absence of any activity of soluble CA in plasma. This was first described for dog and fish (14) and later for pig, sheep, rabbit, and various fish species (74, 75, 77, 83, 109, 137, 149). The molecular size of this endogenous CA inhibitor was determined to be 10–30 kDa for the eel (74) and 79 kDa for the pig (148).

In view of the presence of an extracellular membrane-bound CA activity available to plasma in lung and muscle, the existence of a plasma CA inhibitor seems astonishing. However, some experiments indicate that the plasma inhibitor inhibits erythrocytic cytosolic CA rather

well, but CA from lung tissue homogenate (membrane-bound CA; dog) only incompletely (83). Similarly, plasma inhibitor from pigs showed a less than complete inhibition of vascular CA activity in lungs of rats (78), where the vascular activity of CA is known to be CA IV located on the extracellular luminal surface of capillary endothelial cells.

It may be hypothesized that, due to its molecular size, the plasma inhibitor has no access to the interstitial space. Thus a CA associated with the sarcolemma may be left uninhibited by the plasma inhibitor, because a macromolecule of this size may not enter the interstitial space to a great extent. Even the endothelial membrane-bound CA IV in the lung appears to be only partly inhibited, and this should also be true for capillary CA IV of muscle (and, for example, of the brain).

We conclude that the plasma inhibitor will inhibit erythocytic CA released from any hemolyzed red blood cells throughout the blood vessels rather completely, thus reducing the dehydration/hydration reaction in the plasma to the uncatalyzed velocity, whereas in vascular regions with a membrane-bound CA, e.g., muscle, heart, lungs, and others, a marked catalysis of the dehydration/hydration reaction can take place even in the presence of a plasma inhibitor. Thus CA activity available to plasma appears to be confined to precise localizations within the circulation that are equipped with a capillary CA.

The effect of presence of CA in the plasma has been studied by Wood and Munger (186) for the rainbow trout. They found that CA attenuated postexercise increases in P_{CO_2} and decreases in arterial pH by producing an increase in CO_2 excretion during exercise. However, the normal postexercise hyperventilation was also greatly attenuated when CA was present in the plasma, as was the normal increase in the plasma levels of epinephrine and norepinephrine. They concluded that CO_2 is an important secondary drive to ventilation in fish, and by increasing CO_2 excretion by the presence of CA in the plasma this drive is diminished. The plasma CA inhibitor will ensure that no CA activity of hemolysed erythrocytes is present and thus will contribute to maintain a high level of ventilation in certain situations, which will be favorable for O_2 supply.

E. Interconversion Between CO_2 and Carbamate

The kinetics of oxylabile carbamate was thoroughly reviewed by Klocke (105). We only briefly summarize the relevant facts in these sections.

1. In plasma

The kinetics of this interconversion do not seem to be important for overall CO_2 kinetics, since venous and arterial plasma carbamate concentrations are almost identical. The kinetics of plasma carbamate formation were characterized by Gros et al. (61) by a half-time of this reaction of 0.047 s.

2. In erythrocytes

The binding of CO_2 to hemoglobin in solution has long been known to be quite rapid, requiring a time to reach completion of 0.1–0.2 s (44), which corresponds to a half-time of ~0.04 s. Gros et al. (68) have studied the kinetics of hemoglobin carbamate formation in a wide range of pH and P_{CO_2} values using a pH stopped-flow technique. They determined kinetic constants for the forward reaction of amino groups and CO_2, k_a, for the α-chain and the β-chain α-NH_2 groups in addition to the e-NH_2 groups of human oxy- and deoxyhemoglobin. Table 5 shows the complete set of constants reported by Gros et al. (68) with k_a, pK_z, and pK_c, which describe their kinetic measurements. With these constants, overall carbamate kinetics under physiological conditions of pH and P_{CO_2} were estimated to possess a half-time of 200 ms and to require ~1 s to reach equilibrium by 95%. Their measurements were performed in the absence of 2,3-DPG, and these times may become slightly shorter when 2,3-DPG is present. Nevertheless, their estimate of the half-time of carbamate formation is considerably greater than that of Forster et al. (44) but is similar to Klocke's estimate (102) of the half-time of mobilization of oxylabile carbamate of 0.12 s, which was obtained in the presence of 2,3-DPG.

III. CARBON DIOXIDE TRANSPORT IN MUSCLE

A. CO_2 Production in Muscle

Unlike most other tissues, muscle exhibits a vast range of aerobic (and anaerobic) metabolic rates. In humans, O_2 consumption of muscle tissue can rise 15- to 20-fold from resting values of ~10 μmol·min^{-1}·100 g^{-1}, and even higher increases have been reported from 6.3

TABLE 5. *Velocity constants, k_a, and equilibrium constants for carbamate reactions of human hemoglobin*

	α-Chain α-NH_2	β-Chain α-NH_2	ϵ-NH_2
Oxyhemoglobin k_a, $M^{-1} \cdot s^{-1}$	660	430	14,600
pK_z oxy	6.72	6.42	10.45
pK_c oxy	5.58	5.00	5.07
Deoxyhemoglobin k_a, $M^{-1} \cdot s^{-1}$	4,320	1,040	8,800
pK_z deoxy	7.32	6.35	10.45
pK_c deoxy	5.04	4.39	5.03
Number of amino groups	2	2	44

Experimental conditions are as follows: 37°C, 0.15 M NaCl, absence of 2,3-DPG (68, 69).

mmol·min^{-1}·100 g^{-1} at rest to 200 μmol·min^{-1}·100 g^{-1} at maximal exercise of a small muscle group (forearm; Ref. 73). Carbon dioxide production rates can be calculated from these O_2 consumption rates using a RQ of ~0.85. The P_{CO_2} values in the venous blood leaving the skeletal muscle have also been measured and are ~5.32–5.99 kPa (40–45 mmHg) at rest and can rise to as much as ~13.3 kPa (100 mmHg) during exercise (for example, Ref. 95).

Although different muscle types and different mammalian species have vastly different maximal specific O_2 consumption rates, maximal specific mitochondrial O_2 consumption differs considerably less. At maximum O_2 consumption ($V_{O_{2max}}$), mitochondria of different species consumed 4.56 ± 0.61 ml O_2·min^{-1}·ml^{-1} (87). This indicates that it is essentially mitochondrial density in muscle fibers that determines maximal specific O_2 consumption of these fibers.

Carbon dioxide produced within muscle mitochondria has to diffuse through the intracellular compartment and cross the sarcolemmal membrane and the capillary wall to reach the convective medium blood. Because all the membranes crossed by CO_2 along this diffusion pathway are considered highly permeable to CO_2, their surface area is of no relevance for CO_2 transport, but this area may be important for the permeation of ions associated with gaseous exchange. Among these membrane barriers, the capillary wall has by far the smallest surface area, only ~1/5 of the entire area of the sarcolemma (185) and only ~1/200 of the total area of the inner mitochondrial membranes (87). The following fluxes of respiratory gases occur across the surface of the capillary wall. Maximal flow of O_2 per area of capillary wall is 1.3–1.9 μl O_2·min^{-1}·cm^{-2} as calculated from Conley et al. (20), where the higher values have been measured in more athletic species (dog, pony) and the lower values in less athletic ones (goat, calf). Corresponding maximal total CO_2 flux across capillary wall can be expected to be ~15% lower than the respective O_2 fluxes (~60 nmol CO_2·min^{-1}·cm^{-2}). The area of inner mitochondrial membranes being larger, CO_2 flux across this membrane is expected to be ~0.3 nmol CO_2·min^{-1}·cm^{-2}. This may indicate that the capillary wall could be a significant barrier to ion fluxes associated with CO_2 transport.

B. Localization of CA in Skeletal Muscle

As discussed for erythrocytes, dissolved CO_2 gas with few exceptions is highly permeable across biological membranes, but the more abundant species, HCO_3^-, is not. This permeability difference requires conversion of HCO_3^- to CO_2 at a sufficient speed in red blood cells as well as in muscle cells before permeation of the membrane occurs, and only CA can ensure this rapid conversion.

Several types of CA are present in various parts of skeletal muscle as has been reviewed by Gros and Dogson (60) and recently by Henry (79). Table 6 gives a summary of CA localizations in skeletal muscle.

1. Capillary endothelium

As discussed in section II*D*, there is clear evidence that skeletal muscle capillaries possess an endothelial membrane-bound CA. The evidence that this enzyme is CA IV appears convincing.

2. Sarcolemma

Carbonic anhydrase associated with this membrane was found with a variety of methods. The first evidence for the presence of an extracellular catalysis of the hydration/dehydration reaction in the capillary bed of skeletal muscle arose from functional studies. From observation of the distribution space of $H^{14}CO_3^-$ and its reduction in the presence of CA inhibitors, it was concluded that an extracellular CA in mammalian skeletal muscle exists (38). Its inhibition properties were different from those of the cytosolic enzymes, and it was concluded that this isozyme is present in the interstitial space and probably bound to the sarcolemma (50, 51). Other functional stud-

TABLE 6. *Localization of carbonic anhydrase in skeletal muscle*

Localization	CA	Fiber Type	Species	References
Capillary wall	CA IV	All	Rat, human	157
Sarcolemma	CA IV	All	Rabbit, rat, human	24–26, 50, 175, 179
Cytosol	CA III	Slow oxidative	Human, rabbit, rat, cat, pig, ox	see review, Ref. 60
	CA II	Fast glycolytic	Rabbit, frog	155, 161
		Slow oxidative	Absent in rat	54
			Absent in mouse	21
	CA		Crayfish	151
Sarcoplasmic reticulum	CA IV	All	Rabbit, rat,	17, 24
Mitochondria	CA V		Present in guinea pig	165
			Absent in rabbit, rat, and mouse	17, 124

CA, carbonic anhydrase.

ies have indicated that an extracellular CA available to plasma is involved in fast pH equilibration of the venous effluent and the interstitial space. With the use of a stop-flow technique, it was shown that an electrolyte perfusate had access to a CA while it passed through the hindlimb capillary bed. By inhibiting this extracellular CA, a pH disequilibrium developed in the venous saline perfusate, and the pH of the effluent slowly became more acidic after the saline had left the capillary bed, i.e., a so-called postcapillary acid pH shift developed (129). It appears likely now that these effects, at least partly, are due to capillary endothelial CA IV.

Transient changes of surface pH, induced by sudden addition and withdrawal of propionic acid, were magnified when CA was inhibited in isolated soleus muscle from mouse and rat and in cardiac muscle from sheep, rabbit, and cat (25). Transient changes of surface pH induced by a sudden increase and decrease of P_{CO_2} were blocked by CA inhibitors in a nonvertebrate muscle, the crayfish muscle (151). In the former case, surface pH change is due to a net movement of H^+ across the membrane together with propionate. When sarcolemmal CA is blocked, the efficacy of the CO_2/HCO_3^- buffer is diminished, producing an increased pH transient. In the latter experiment, inhibition of the sarcolemmal CA activity leads to a suppression of surface pH transients that are caused by net fluxes of CO_2, which go along with rapid changes in surface P_{CO_2} that are followed by H^+ production or consumption when CA is present on the cell surface, but are not (or very slowly) when CA is inhibited. These effects are clearly due to a CA bound to the external surface of muscle fibers.

In sarcolemmal vesicles, a CA was found in preparations from red and from white muscles of the rabbit. The inhibition constants (K_i) of this sarcolemmal CA toward acetazolamide, chlorzolamide, and cyanate were shown to be different from those of CA II or CA III (179). With CA IV antibodies this sarcolemmal CA was identified to be CA IV (175). In semithin and ultrathin sections of rat soleus muscle, CA IV was found immunocytochemically to be associated with the sarcolemma in addition to its association with the capillary endothelium and the SR (24). In mammalian heart, CA IV was also found to be associated with the sarcolemma in addition to the capillaries (156). Thus the present state of information indicates that sarcolemmal CA is the membrane-bound, glycosyl-phosphatidylinositol (GPI)-anchored isoform CA IV.

3. Cytoplasm

It is well known that the sulfonamide-resistant isozyme CA III is present in high concentration in the cytoplasm of mammalian skeletal muscle type I (slow-oxidative fibers) (review, Ref. 60). A sulfonamide-sensitive CA, probably CA II, was found in the cytosol of white muscles of the rabbit (161) and in the mouse soleus (21). In the latter case, however, no measurements of the erythrocytic contamination of the muscle homogenates were done; thus CA II of erythrocytes could be present in these experiments. In contrast, in the former case, red cell contamination was carefully controlled. In the cytoplasm of white as well as red hindlimb muscles of the rat, no sulfonamide-sensitive CA was present (54). For other animal groups, studies are scarce; from functional studies, the presence of a CA in the cytosol of crayfish muscle was deduced (151), and there is one report indicating that frog white muscle has a CA II-type isozyme (155).

Mammalian heart muscle appears to contain no cytosolic enzyme but high activities of the membrane-bound form (17, 54).

4. SR

A membrane-bound CA was detected in preparations of SR vesicles from red as well as white skeletal muscle of the rabbit (17). This finding was confirmed by histochemical results employing the fluorescent CA inhibitor dansylsulfonamide for CA staining (17, 26). Although it has not been possible to visualize SR-CA immunocytochemically at the light microscopic level (157), membrane-bound CA IV was found to be associated with SR by electron microscopy and use of CA IV antibodies (24). This latter finding corresponds with a reaction of SR membranes with anti-CA IV in Western blots (175). Wetzel and Gros (180) have found that nevertheless the inhibitory properties of the CA of SR toward sulfonamides are significantly different from those of the CA of the sarcolemma, which may indicate either that SR-CA is an isoform somewhat different from CA IV or has different properties because of a different membrane environment. In the mammalian heart, immunocytochemical evidence at the electron microscopic level indicates that CA IV is also associated with the SR (156).

5. Mitochondria

Mitochondrial CA, CA V, is present in high activities in liver and kidney mitochondria (see review, Ref. 60). In skeletal muscle, mitochondrial CA was found only in muscles of the guinea pig but was not detectable in skeletal muscles of the rabbit or the rat or the mouse (Table 6). Carbonic anhydrase V has been detected in immunocytochemical studies in the mitochondria of rat skeletal muscle in addition to those in several other rat tissues (174). However, these results were dependent on an antibody that misidentified another antigen in rat mitochondria as CA V. Ohliger et al. (130) reported that malate dehydrogenase copurified with rat CA V on the inhibitor affinity column used to purify rat liver CA V for the production of the antibody. Thus the antibody used may have recognized malate dehydrogenase rather than CA V.

Thus it appears that CA V is absent in skeletal muscle mitochondria of several species.

From experiments with mitochondria of mammalian liver, it is known that mitochondrial CA V rapidly provides HCO_3^- for reactions in ureagenesis and in gluconeogenesis (31, 32). Whereas the former is not known to occur in muscle, gluconeogenesis does occur to some extent in this tissue. When intact hepatocytes were incubated under conditions in which gluconeogenesis begins with HCO_3^- fixation via pyruvate carboxylase (high lactate/pyruvate concentrations), treatment with CA inhibitors decreased glucose synthesis (31). Such a role for mitochondrial CA V was found in rat kidneys as well (33).

Balboni and Lehninger (5) compared CO_2 uptake by rat liver mitochondria, which possess CA, with heart mitochondria, which do not (34). In the liver a rapid net uptake of CO_2 was found in association with K^+ or Ca^{2+} entry. It was concluded that by rapid hydration inside mitochondria H^+ were provided to act as counterion for these cations. In the heart, no net uptake of CO_2 was found using the same experimental conditions, and it was concluded that CA is not present in mitochondria of rat heart.

In contrast to these findings, Nagao et al. (124) found CA V in the mitochondria of heart muscle in rat but not in mouse. Their finding is based on CA V-specific antibodies obtained by immunizing rabbits against the COOH-terminal peptides predicted from the mouse and rat CA V cDNA.

C. Transport in the Intracellular Compartment

1. CO_2 elimination and facilitated diffusion

Diffusion of CO_2 in the intracellular compartment includes diffusion of dissolved and bound CO_2, as has been discussed for erythrocytes.

Diffusion coefficients of dissolved CO_2 measured within intact muscle cells in the sarcoplasm are not available, but for a number of small molecules and ions such as potassium, sodium, sulfate, and sucrose, it has been shown that the diffusion coefficients in the sarcoplasm were reduced by a factor of 2 compared with those in aqueous solutions (107). This would predict a CO_2 diffusion coefficient in the sarcoplasm of $\sim 8 \times 10^{-6}$ cm^2/s at 22°C and $\sim 1.3 \times 10^{-6}$ cm^2/s at 37°C. Such a value would roughly agree with what is predicted by the relation between CO_2 diffusion constant and protein concentration given in Figure 2.

Carbon dioxide diffusion was, however, measured across layers of intact skeletal muscle tissue including sarcolemmal membranes, and in these experiments, the diffusivity of dissolved CO_2 and the contribution of facilitated diffusion to overall CO_2 transport was estimated. From the data of Kawashiro and Scheid (97), a diffusion coefficient D of 1.19×10^{-5} cm^2/s ($K = 2.93 \times 10^{-4}$ cm^2·min^{-1}·atm^{-1}) at 37°C can be derived for plain diffusion of dissolved CO_2 in rat abdominal muscle. When facilitated diffusion was present in their experiments, i.e., in the lower range of CO_2 partial pressures, the diffusion coefficient was increased by a factor of >2. Similar facilitation factors were reported for rat abdominal muscle at 25°C (60). When facilitation was suppressed by inhibition of CA, a diffusion constant K of 3.8×10^{-4} cm^2·min^{-1}·atm^{-1} was measured, and this value increased to 6.5×10^{-4} cm^2·min^{-1}·atm^{-1} in the absence of the CA inhibitor. Similar contributions of facilitated diffusion were measured for other skeletal muscle types by Romanowski et al. (143). Table 7 shows their data in which the ratio Q of CO_2 diffusion constant over acetylene diffusion constant, which is 0.9 for diffusion of the dissolved gases only, has been determined for muscle sections from heart, soleus, extensor digitorum longus, masseter, and gracilis muscles of the rabbit and for abdominal muscle of the rat. In all these muscles, the ratio Q is greater than 0.9, indicating that a facilitation of CO_2 diffusion increases intracellular CO_2 transport between 2- and 3.7-fold. Thus it appears well established that at normal intracellular pH values, intracellular CO_2 transport is significantly accelerated by facilitated CO_2 diffusion. The requirement of CA in the intracellular space for this process is evident from the inhibitory effect of acetazolamide on facilitation in all muscles studied (Table 7). Because facilitation occurs even in heart muscle, which has no cytosolic CA, it appears that part of the necessary catalysis is mediated by intracellular membrane-bound CA as discussed above (e.g., SR CA). This shows that the intracellular presence of CA in muscle is useful for CO_2 elimination from the muscle cell, which is in contrast to Roughton's (146) remark that in a tissue such as muscle "carbonic anhydrase is an enemy to the organism rather than a friend,"

TABLE 7. *Facilitated diffusion in muscles*

Muscle	Q, cm^2 · min^{-1} · atm^{-1}			Facilitation Factor
	Control	pH 4	Acetazolamide	
Heart	2.4 ± 0.4	0.9 ± 0.2	1.3 ± 0.2	2.7
Soleus	3.1 ± 0.4	0.9 ± 0.2	2.0 ± 0.2	3.5
EDL	1.9 ± 0.3	0.9 ± 0.1	1.0 ± 0.1	2.2
Masseter	1.9 ± 0.3	0.9 ± 0.1	1.4 ± 0.2	2.0
Gracilis	2.9 ± 0.6		1.3 ± 0.1	3.2
Abdominal muscle*	3.4 ± 0.3		1.1 ± 0.1	3.7

Quotients (Q) of diffusion constants K_{CO_2} over $K_{acetylene}$ for various muscles from the rabbit or rat (*). Control, after 45-min preincubation in Ringer solution, pH 7.4; pH 4, after preincubation in isotonic sodium lactate of pH 4.0; acetazolamide, after preincubation in Ringer solution, pH 7.4, with 1×10^{-3} to 6×10^{-3} M acetazolamide. Facilitation factor is Q(control)/Q(pH 4) and represents a factor by which CO_2 transport is accelerated due to facilitation. EDL, extensor digitorum longus muscle. [Data from Romanowski et al. (143).]

because it would rapidly convert the membrane-permeable CO_2 into the impermeable HCO_3^- and thus impair CO_2 elimination.

Facilitated diffusion is based on diffusion of HCO_3^- and H^+/buffered H^+, respectively, occurring in parallel to diffusion of free CO_2. The potential contribution of facilitated diffusion to overall diffusion depends on the ratio of HCO_3^- to dissolved CO_2 and, thus, depends on the actual pH in muscle cytoplasm (in addition to dependence on the concentration of mobile buffers and the presence of CA activity). In heavily exercising muscle, in addition to CO_2, lactic acid is produced and the additional H^+ shift the equilibrium of the hydration/dehydration reaction toward CO_2 and have to be buffered and eliminated from the cell. Intracellular pH of skeletal muscle can become very low and can decrease from ~7.2 at rest to a value as low as 6.6–6.7 (6, 110) or to even lower values of 6.2–6.4 (119, 152, 183) during maximal exercise. Accordingly, during maximal work, HCO_3^- concentration is only two times that of dissolved CO_2, whereas during rest, the ratio of HCO_3^-/CO_2 is ~13. As a result, less facilitation of CO_2 diffusion can be expected to take place during heavy exercise. At the same time, the "CO_2 store" in the muscle, HCO_3^-, will be mobilized by the intracellular metabolic acidosis producing high P_{CO_2} values in muscle tissue and in the venous blood leaving the exercising muscle.

2. H^+, lactic acid, and lactate diffusion

The substantial facilitation of CO_2 diffusion in muscle as seen in Table 7 implies that the muscle cell possesses a highly effective mechanism of intracellular H^+ transport by diffusion of mobile buffers. As judged from the facilitation factors given in Table 7, this H^+ transport mechanism is at least two times more efficient than the 66 mM phosphate buffer at pH 7 as used in Figure 3. Although there are no data on intracellular lactate diffusivity, it is expected that lactate has a diffusion coefficient similar to that estimated above for HCO_3^-. This has the following implication. The intracellular H^+ transport capacity, which suffices to transport H^+ at a rate equal to the rate of HCO_3^- transport as it results from a HCO_3^- concentration difference in the millimolar range (facilitated CO_2 diffusion), will also suffice to transport H^+ at a rate equaling the lactate flux that results from a lactate concentration difference in the millimolar range (lactic acid transport). Thus lactic acid, which is almost completely dissociated at physiological pH values, can be efficiently transported through the cell interior utilizing this facilitated H^+ transport system. It may be noted that this H^+ transport system under conditions of exclusively aerobic metabolism is used by the cell to maintain a facilitation of CO_2 diffusion, whereas under conditions of dominating anaerobic glycolysis and low intracellular pH, it is mainly used to transport H^+ along with the lactate anion through the intracellular space, a prerequisite for the elimination of lactic acid from the cell.

3. CO_2 and Ca^{2+} mobilization in the SR

There is considerable evidence that H^+, in addition to Mg^{2+} and K^+, acts as a counterion when Ca^{2+} moves across the sarcoplasmic membrane during Ca^{2+} release and reuptake (116, 117, 164). In view of the abundance of CO_2 in the cell and its high permeability in membranes, CO_2-HCO_3^- seems to constitute an ideal buffer system within the SR able to produce or buffer H^+. Without CA, the CO_2 hydration reaction has a half-time of ~10 s. This is by far too slow in view of the rapid Ca^{2+} movements across the SR membrane that have half-times of 10–100 ms. Bruns et al. (17) have postulated that the CA of the SR may act to provide a rapid source and sink for H^+ to be exchanged for Ca^{2+} across the SR membrane as illustrated in Figure 4. Carbonic anhydrase activity associated with the SR was calculated to accelerate the reaction 500- to 1,000-fold, thereby reducing the half-time to 10–20 ms. In view of the small SR-to-cytoplasm volume ratio, they postulated that this buffering mechanism would have to be more efficient in the interior of the SR than outside. From studies with SR vesicles, it could be shown that a major part of the SR CA activity is indeed catalytically active in the interior of the SR (55; G. Gros, S. J. Dodgson, E. A. Haller, B. T. Storey, and R. E. Forster, unpublished observations). By inhibiting this CA, one would expect to interfere with the rapid H^+ exchange and thus to slow down Ca^{2+} release and reuptake. By measuring Ca^{2+} transients in skeletal muscle fibers with the Ca^{2+} indicator fura 2, Wetzel et al. (181) showed indeed that CA inhibition slows down Ca^{2+} release as well as Ca^{2+} reuptake by the SR. Geers and Gros (52, 53) showed that, as a consequence, CA inhibition of skeletal muscles results in a prolongation of time-to-peak and of half-relaxation time during isometric contraction. This constitutes an example in skeletal muscle, where the abundant presence of CO_2 in the tissue is utilized for a process resembling H^+ secretion in other organs.

D. Transport Across Sarcolemma

As discussed for the red cell membrane, it seems reasonable to assume that the bulk of CO_2 crosses the sarcolemmal membrane in the dissolved form. On the other hand, because HCO_3^-/Cl^- exchange is known to be involved in pH regulation of muscle cells (1), HCO_3^- permeability constants can be expected to be higher than those for lipid bilayers, and the estimate of 2×10^{-7} cm/s given by Woodbury and Miles (188) for frog skeletal muscle appears surprisingly low (see Table 3).

Transport of bound CO_2 in the form of HCO_3^- across sarcolemma is closely linked with other processes in-

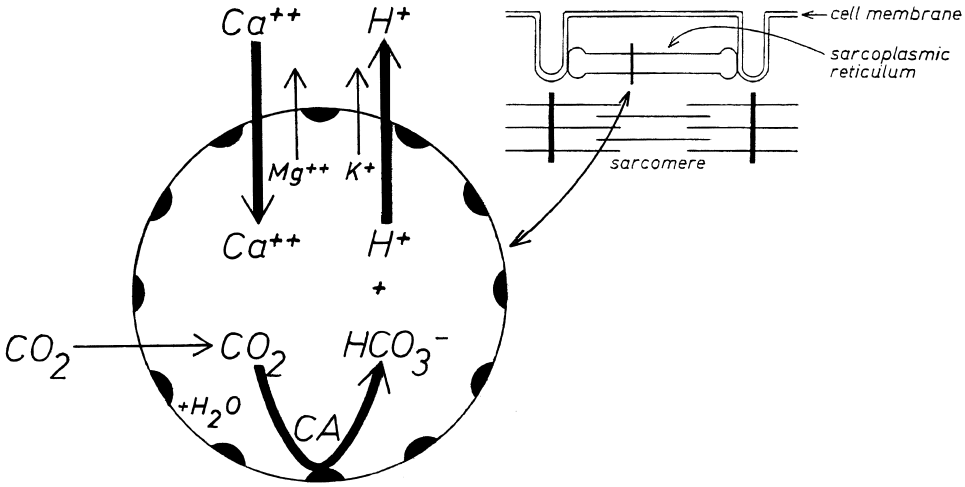

FIG. 4. Schematic representation of proposed role of sarcoplasmic reticulum (SR) carbonic anhydrase (CA) in Ca^{2+} transport across the SR membrane. Catalyzed CO_2 hydration within the SR provides protons that are exchanged for Ca^{2+} across SR membrane. Ca^{2+} uptake requires rapid H^+ production within SR, as shown; Ca^{2+} release requires rapid H^+ buffering. Other counterions of Ca^{2+} appear to be Mg^{2+} and K^+. As indicated at *right*, scheme on *left* is projected into a cross section through SR or L system. [From Geers et al. (55).]

volved in pH regulation. Bicarbonate is in equilibrium with CO_2 and H^+, whose concentration in turn is dependent on production of lactic acid and H^+ removal from the cell. Figure 5 shows three transport mechanisms that are involved in pH regulation of vertebrate muscle cells and how they are linked to CO_2 excretion of the cell. The transport mechanisms were reviewed by Aickin (1), and the contribution of lactate-H^+ cotransport to pH regulation was evaluated by Juel (94).

pH regulation has been observed by measuring the rate of recovery from intracellular acidification. With the study of the effects of the presence of either SITS/DIDS or of the virtual absence of CO_2, the contribution of HCO_3^-/Cl^- exchange was assessed. Observing the effect of the presence of amiloride the contribution of Na^+/H^+ exchange to pH regulation could be evaluated. At rest, predominantly Na^+/H^+ exchange and probably to a smaller extent HCO_3^-/Cl^- exchange are responsible for pH regulation (Table 8; see review in Ref. 1).

During exercise, however, when indeed huge amounts of H^+ are produced by anaerobic glycolysis inside muscle cells making highly efficient pH regulation vital, the relative contribution of these two pH-regulating mechanisms is drastically reduced. Syme et al. (168) observed that the increase in fixed acid concentration in the cytosol of the plantaris-gastrocnemius-soleus muscle group by sciatic nerve stimulation was unchanged either by the presence of DIDS or by an additional increase in CO_2. The authors concluded from this that HCO_3^-/Cl^- exchange is not important for pH regulation during this condition of heavy exercise. This seems quite compatible with the idea that during exercise lactate-H^+ cotransport is the predominant contributor to pH regulation. Westerblad and Allen (178) found that inhibition of lactate-H^+ transport had an effect on intracellular pH only during exercise but not during rest. That during exercise this transporter carries the major load of acid extrusion was shown by studies with sarcolemmal vesicles by Juel (92, 94). Lactate-H^+ cotransport has by far the highest capacity to remove H^+ from the muscle cell, and this is even more obvious for slow oxidative fibers than for fast glycolytic ones (Table 8; Ref. 92). For zero-*trans*-condition in vesicles, Juel (91) found a maximum velocity value for lactate-H^+ cotransport of 48 pmol·s^{-1}·cm^2 sarcolemmal surface^{-1} at room temperature. With a Q_{10} value of 2.2 (91), this becomes ~160 pmol·s^{-1}·cm^{-2} at body temperature. This lactate-H^+ cotransporter is strongly dependent on pH. With an acidic pH in the interstitial space, the efflux of lactic acid from the muscle cell would be slowed down. Juel (93) found a steep pH dependency, predicting that a decrease of pH by 1 unit on one side of the membrane decreases lactate flux in this direction to 20%.

Let us consider a situation of heavy exercise inside and outside the sarcolemmal membrane. In Figure 5, values are given for pH, P_{CO_2}, HCO_3^-, and lactate as they may be present after an intense exercise period of skeletal muscle. They were taken in this example for sarcoplasm from Bangsbo et al. (6), and values for the interstitial space were assumed to be similar to venous values. The P_{CO_2} is assumed to be instantaneously equilibrated across the sarcolemma and therefore assumed to be identical in the sarcoplasm and the interstitial space. There is no "facilitated CO_2 diffusion" across the sarcolemma, i.e., HCO_3^- does not contribute to CO_2 excretion of the cell. The reason for this is not only the low membrane permeability for HCO_3^- compared with that for dissolved CO_2, but also the contribution of HCO_3^-/Cl^- exchange to acid extrusion, which operates in the "wrong" direction. To be effective for pH regulation and acid extrusion, HCO_3^- has to enter the cell, buffer H^+, and after conversion to CO_2 leave the cell in the form of dissolved gas. The gradient for HCO_3^- into the cell, especially during intense exercise, is large, because intracellular pH is much lower than extracellular pH (Fig. 5). Thus no net excretion of CO_2-HCO_3^- from the cell is contributed by the $HCO_3^-/$

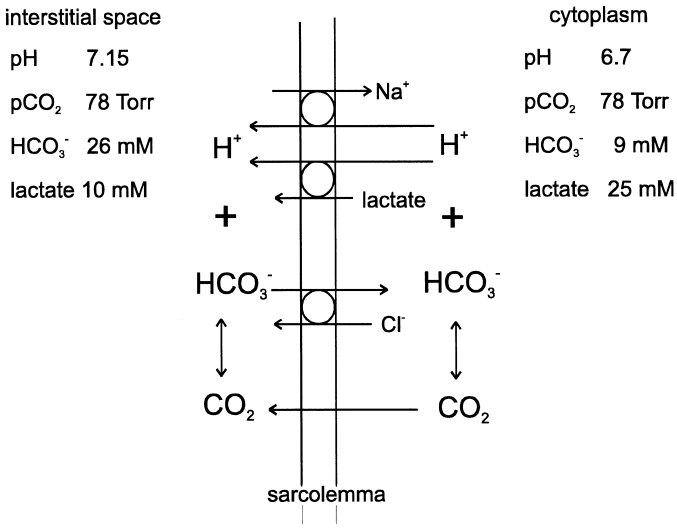

FIG. 5. Reactions and transport processes involved in pH regulation of the muscle cell.

Cl^- exchange. The high concentration of HCO_3^- in the interstitial space in this situation is useful because it provides a high buffer capacity for H^+ leaving the muscle cells by lactate-H^+ cotransport or Na^+-H^+ countertransport. The consumption of extracellular HCO_3^- in the interstitial space by lactic acid producing cells (Fig. 5) is likely to be an important mechanism allowing H^+ efflux from the cell to be maintained. However, for this process to be sufficiently fast, CA is probably mandatory, and the extracellular sarcolemmal CA would appear to be an ideal enzyme to make the buffer capacity of interstitial HCO_3^- fully and rapidly available. Without this enzyme, interstitial pH can be expected to become much lower, and this may slow down lactate-H^+ cotransport (see Fig. 5). Indeed, Kowalchuk et al. (106) have observed that the postexercise increase in lactate concentration in the blood was significantly lower after treatment with acetazolamide, and Geers et al. (49) have found that inhibition of extracellular muscle CA causes a decrease of lactate release from moderately exercising isolated blood-perfused muscle.

E. Transport Across Capillary Walls

Among all the surface areas that CO_2 and HCO_3^- as well as H^+ and lactate have to cross, the capillary wall has the smallest surface with only approximately one-fifth of that constituted by sarcolemma (185). Permeability coefficients for CO_2 are expected not to be different from those measured for lipid bilayers or the erythrocyte membrane, but direct measurements are not available. The capillary wall is known (see review in Ref. 120) to possess water channels. For skeletal muscle capillaries it was shown that these channels have pore sizes of around ~4 nm (177). This author estimated that 60% of the hydraulic capacity of cat skeletal muscle capillaries represents a "water-only pathway." This pathway may be one of the aquaporins, which has been shown to be present in skeletal and cardiac muscle capillaries (125). On the other hand, Michel (120) postulated that through >90% of the capillary water channels not only water is able to flow, but in addition small solutes are allowed to pass through. HCO_3^-, H^+, and lactate would be classified as such small hydrophilic solutes and then could cross this barrier not only by diffusion but also by convection. Thus capillary wall permeability for HCO_3^-, H^+, and lactate can be expected to exceed that of sarcolemma. However, no direct permeability measurements for either CO_2, HCO_3^-, H^+, or lactate are available for capillary walls.

Capillary wall diffusion capacity for small solutes has often been measured as permeability-surface area product (*PS*) for substances with molecular weights similar to lactate (mol wt 89) and HCO_3^- (mol wt 61). The *PS* for Na^+ (mol wt 23) was reported to be 21 ml·min^{-1}·100 g^{-1} for cat skeletal muscle capillaries (177). The *PS* for EDTA (mol wt 341) of rat skeletal muscle was 12.9 ml·min^{-1}·100 g^{-1} (72). Assuming a capillary surface area of 7,000 cm^2/100 g (132), these authors calculated from this value an EDTA permeability of 3×10^{-5} cm/s, and a similar value was reported by Michel (120). Using the same capillary surface area, Watson's (177) results for Na^+ give a capillary Na^+ permeability of 5×10^{-5} cm/s. With their own measurements of capillary density, Shibata and Kamiya (159) found a very much lower permeability of rabbit skeletal muscle capillaries for EDTA of only 6×10^{-6} cm/s. In view of possible convection through water channels in addition to diffusion, these permeability values for Na^+ and EDTA are astonishingly low compared with the permeabilities of the erythrocyte membrane, which, for the anion HCO_3^- for example, is one order of magnitude higher (5.6×10^{-4} cm/s; Ref. 160).

TABLE 8. *Relative contribution of different mechanisms to pH regulation of muscle cells*

Na^+/H^+	HCO_3^-/Cl^-	$Lactate^-/H^+$	Muscle Cells	References
		At rest		
80%	20%		Mouse, soleus	1, 2
~50%	~50%		Mouse, EDL	70
80%	20%		Rat, diaphragm	144
		Exercise condition, lactic acidosis		
	In vivo not important		Rat, hindlimb muscle	168
10%	17%	73%	Rat, red muscles	92
12%	16%	72%	Rat, white muscles	92

EDL, extensor digitorum longus muscle.

IV. KINETIC REQUIREMENTS OF THE PROCESSES INVOLVED IN ELIMINATION OF CARBON DIOXIDE AND LACTIC ACID FROM MUSCLE AND UPTAKE INTO BLOOD

Figure 6 illustrates the processes involved in CO_2 and lactic acid transfer from the cytoplasm of muscle cells to plasma and into the interior of erythrocytes, as discussed in sections I–III. What is the role of these processes for the overall kinetics of CO_2 uptake into red blood cells and lactic acid transfer into the blood? Table 9 shows the times required for 95% completion of CO_2 uptake if any one of these single processes would determine the kinetics of the overall process. Table 9 gives a rough idea of how critically each process will affect the overall time course. The theoretical model of CO_2 and lactic acid exchange presented in section IV*A* analyzes the role of each process quantitatively.

TABLE 9. *Time required for equilibration after CO_2 and lactic acid release from skeletal muscle*

Process Limited by	Time (95%), ms
Buffering of H^+	Instantaneous
Intracellular CO_2 diffusion	6
CO_2 permeation of red cell membrane + diffusion	6
Diffusion of CO_2 from muscle to plasma	?
Velocity of intraerythrocytic CO_2 hydration (14,000 fold accelerated, A = 14,000)	2
HCO_3^-/Cl^- exchange (182)	430–500
Carbamate reaction (69, 102)	500
Permeation of lactate or HCO_3^- through capillary wall (with assumed permeability of 0.0002 cm/s)	1,000
Extracellular CO_2 hydration in plasma	
Without CA activity [$t_{1/2}$, 8 s; (57)]	34,000
100-fold accelerated (A = 100)	340
Uptake of lactic acid in red blood cells [$t_{1/2,effluent}$, 35 s; (91)]	150,000

Where included, reference numbers are given in parentheses. $t_{1/2}$, half-time.

A. Theoretical Model of CO_2 and Lactic Acid Exchange in Muscle

To understand the complex interdependence of reactions and transport processes involved in CO_2 exchange more completely, we will use a theoretical model. An analysis of postcapillary pH equilibration and the role function of CA therein has been presented primarily for the gas exchange in the lung (10, 45, 84). The following reasons prompted us to thoroughly modify existing models for the situation in skeletal muscle instead of merely extrapolating from the lung models.

1) In skeletal muscle not only CO_2 exchange but also release of lactic acid from muscle tissue has to be considered, since this represents another disturbance of pH equilibration. Lactic acid is not considered in lung models, whereas this appears necessary for skeletal muscle.

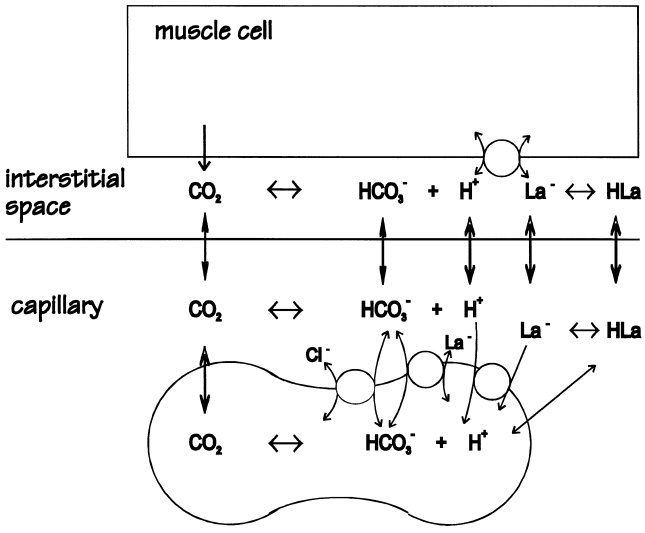

FIG. 6. Reactions and transport processes included in the mathematical model (see text).

2) With a model consisting of only two compartments (erythrocytes and plasma), as has been used in the lung models, we were not able to simulate the direction of the postcapillary pH shift measured in isolated blood-perfused rat hindlimb muscle (C. Geers, O. Bertram, and G. Gros, unpublished observations), when extracellular CA was inhibited and CO_2 and lactate were released.

3) Lactate-H^+ cotransport takes place across the sarcolemma; this implies that H^+ are primarily accumulated in the interstitial space and buffering of H^+ by HCO_3^-, the most important buffer in this compartment, will take place there. Thus catalysis of the reaction $HCO_3^- + H^+ \leftrightarrow CO_2$ has to be present in the interstitial space to be useful for the buffering of these H^+. Thus inclusion of interstitial space as another compartment into the model appears indispensable in the case of skeletal muscle.

4) With such a third compartment (erythrocytes/plasma/interstitial space), the functional role not only of an interstitial (sarcolemmal) CA, but also that of a CA inhibitor present in the plasma of a number of species can be studied, since the available evidence suggests that CA is present in each of the three compartments: erythrocytes (cytosolic CA), plasma (CA bound to endothelium), and interstitial space (CA associated with the sarcolemma).

The starting point of the present model was a modified, in some respects (carbamate, deoxygenation) simpler, version of the analysis of postcapillary pH equilibration as it has been described by Bidani et al. (10). We extended this model to include lactic acid exchange and the interstitial space. This model analyzes for steady-state conditions single capillary passages of blood through

muscle tissue and describes the intra- and postcapillary changes of pH, CO_2, HCO_3^-, and lactate in erythrocytes, plasma, and the interstitial space. As an estimate for lactate and CO_2 excretion for a given steady-state condition, muscular arteriovenous concentration differences of lactate and CO_2 were calculated. This model does not describe time-dependent changes in muscle cells or changes in lactate and CO_2 production rates during the onset of exercise.

B. Reactions Included in the Model and Their Mathematical Form

The entire skeletal muscle is thought of as a single unit consisting of muscle cell interior, interstitial space, plasma, and erythrocytes. These compartments are treated as layers with diffusion taking place only perpendicular to the boundaries separating them. Interstitial, erythrocyte, and plasma volumes are given as values relative to blood or capillary volume. The available surface areas of each compartment boundary are given per blood volume and are calculated using estimates of capillary volume-to-skeletal muscle volume ratio (158), hematocrit, erythrocyte surface-to-volume ratio, and a capillary radius of 3.5 μm. Within each compartment molecules are assumed to be always homogeneously distributed. Activity of CA associated with membranes, sarcolemma, and capillary wall was assumed to be homogeneously present in the respective fluid compartment, interstitial space, and plasma. Concentrations inside skeletal muscle cells are assumed to be constant throughout one calculation, although values used are varied to simulate rest or exercise conditions. Blood flow is assumed to be constant. Values for arterial blood entering the capillary are set to standard arterial values; thus for the calculations performed here, these were assumed to be independent of the venous values ("open circuit" system).

During the capillary transit, the blood takes up CO_2, H^+, and lactate from the muscle cell via the interstitial space. Chemical and transport events that occur during gas and lactic acid exchange, which we have included in our calculations, are with few exceptions shown in Figure 6. With steady-state conditions, it is assumed that within each part of the interstitial space along the capillary wall concentrations are constant. Thus the sum of influx and efflux into this compartment and the rate of change of chemical rection has to be zero for CO_2, HCO_3^-, H^+, and lactate. A concentration profile is calculated for these substances parallel to the capillary. For each molecular species, equations describing its rate of change are devised for plasma and erythrocytes, and new concentrations of each substance are calculated at successive points of time, with time intervals <1 ms, as the blood travels along the capillary and until 120 s after it has left the capillary. The mass balance of each molecular species in each compartment considers the rate of consumption and production of that species by chemical reaction within its compartment and/or net transport of the species in and out of the compartment. The reactions and transport events included in the analysis are described as follows. For CO_2, *1*) hydration/dehydration reaction catalyzed by CA or uncatalyzed; *2*) diffusion between skeletal muscle cell, interstitial space, and erythrocytes; and *3*) binding of CO_2 to hemoglobin within erythrocytes (not shown in Fig. 6). For HCO_3^-, hydration/dehydration reaction catalyzed by CA or not (see *point 1*); *4*) diffusion from interstitial space into plasma, and vice versa; and *5*) movement between plasma and erythrocytes via anion exchanger. For H^+, hydration/dehydration reaction catalyzed by CA or not (see *point 1*); *6*) buffered by proteins inside erythrocytes and plasma (not shown in Fig. 6); *7*) cotransport of H^+ and lactate ions across the sarcolemmal and red cell membrane; *8*) release of H^+ by carbamate reaction (not shown in Fig. 6); *9*) uptake of H^+ due to deoxygenation of hemoglobin (not shown in Fig. 6); and *10*) diffusion across the capillary wall. For lactate, cotransport of H^+ and lactate ions across the sarcolemma and erythrocytes (see *point 7*); *11*) movement of lactate ions via anion exchanger between plasma and erythrocytes.

The change of concentration for each species was calculated for interstitial space, plasma, and erythrocytes. The flux of water across the red cell membrane is calculated as described by Bidani et al. (10) using a hydraulic permeability coefficient and the difference in osmolality across the membrane. Table 10 lists the numerical values used for the computations.

C. Permeability of the Capillary Wall to Lactate

Permeability values for lactate across the capillary wall in skeletal muscle are not available. Although the capillary wall has not been considered to form a barrier of functional significance for lactate diffusion (94), one study using microdialysis has demonstrated that interstitial lactate is not always equilibrated with blood plasma lactate (112). Permeability values for muscle capillaries cited for molecules of a size roughly similar to that of lactate (mol wt 89) are 6×10^{-6} cm/s for Cr-EDTA (mol wt 341) in rabbits (159), 3×10^{-5} cm/s for EDTA in rats (72), and depending which capillary surface was used for the calculation $0.5–1 \times 10^{-5}$ cm/s for EDTA in cats (177) and $2–5 \times 10^{-5}$ cm/s for sodium (mol wt 23) in cats (177).

Figure 7 shows that by using these permeability values of the capillary wall for our model calculation we found it impossible to achieve arteriovenous differences for lactate as high as they have been reported to occur. Arteriovenous differences for lactate during and after a

TABLE 10. *Data used in analysis of blood passing through skeletal muscle capillaries*

Half-time of carbamate reaction (103)	0.12 s
Surface area of human erythrocytes/ml blood	~7,800 cm^2/cm^3
Surface area of capillary wall in skeletal muscle/ml blood, calculated for mean capillary diameter of 7 μm [for rat measured, 8,700 cm^2/cm^3 (158)]	5,700 cm^2/cm^3
Surface of sarcolemma/liter blood; ~5 times capillary surface	3×10^4 cm^2/cm^3
Membrane CO_2 diffusion capacity (10)	8.55 mmol $CO_2 \cdot l$ blood$^{-1} \cdot s^{-1} \cdot$ Torr^{-1}
Thickness of erythrocyte membrane	10^{-6} cm
CO_2 hydration velocity constant (147)	0.13 s^{-1}
H_2CO_3 dehydration velocity constant (45)	57.5 s^{-1}
Acid dissociation constant for H_2CO_3 (147)	0.35 mM
CO_2-HCO_3^- equilibrium constant	7.91×10^{-4} mM
Michaelis constant for lactate-H^+ cotransport in skeletal muscle (91)	23.7 mM
V_{max} for H^+-lactate cotransport (37°C)	160 pmol $\cdot cm^{-2} \cdot s^{-1}$
Factor for reduction of V_{max} with pH	to 20% decreased
decrease by 1 unit (93, 94)	
Equilibrium constant for lactic acid	$10^{-3.86}$
Faraday constant	96,480 C/mol
HCO_3^- mobility (using $P = 5.6 \times 10^{-4}$ cm/s for red cell membrane) (160)	2.0×10^{-11} $cm^2 \cdot mV^{-1} \cdot s^{-1}$
Lactate ion mobility across red cell membrane, 10,000 less than for HCO_3^-	2.0×10^{-15} $cm^2 \cdot mV^{-1} \cdot s^{-1}$
Red cell hydraulic coefficient (41)	0.041 cm/s
Buffer capacity in erythrocytes	60 mmol H^+/unit pH
Buffer capacity in plasma	5.5 mmol H^+/unit pH
H^+ taken up due to hemoglobin oxygenation (101)	0.7 mmol H^+/mmol Hb deoxygenated
H^+ taken up due to carbamate formation (8)	1.8 mmol H^+/mmol carbamate formed

Where included, reference numbers are given in parentheses. V_{max}, maximum velocity.

bout of heavy exercise can be as high as 6.6 mM for human skeletal muscle, with intracellular lactate concentration rising to 28 mmol/l cell water and a venous plasma lactate concentration of 14 mM (95).

For example, for a lactate permeability of 2×10^{-5} cm/s, only very low arteriovenous concentration differences for lactate were obtained of $\ll$1 mM, and a prolongation of the transit time to twice the standard value of 1 s for the calculation had only a small effect. The calculated arteriovenous difference becomes only ~2.2 mM, i.e., the venous concentration rises to 4.2 mM from the generally assumed arterial concentration of 2 mM. With this permeability value, the lactate concentration difference across capillary wall can be calculated to be as high as ~12 mM. This would imply that the limiting barrier for lactate excretion is the capillary wall rather than the sarcolemma and would be incompatible with the experimentally obtained arteriovenous lactate concentration differences of 6–7 mM for heavy exercise (95).

On the basis of the calculations shown in Figure 7, it seems clearly warranted to assume a lactate permeability of the muscle capillary of at least 1×10^{-4} cm/s. The calculations with the theoretical model reported below were therefore performed with a capillary permeability for lactate of 2×10^{-4} cm/s. However, with an increase in permeability only the arteriovenous difference is still too low to explain experimental data; thus in addition to this higher permeability value, a longer transit time is probably present in lactate-producing muscle.

The range of muscle capillary transit times reported in the literature is rather wide. Compared with the values in the lung, they were found to be approximately twice as long in a variety of species (98). Values for minimal mean capillary transit times during maximal blood flow under exercise at maximal aerobic capacity were computed from total capillary blood volume/muscle blood flow by Kayar et al. (98) to be 0.7–0.8 s (dog, goat) and 0.8–1.0 s (horse, steers). For humans, a mean transit time of 0.8–0.9 s was estimated at maximal leg exercise (153).

At rest, directly measured red cell transit times across the capillary network were considerably longer, 3–4 s (hamster, cremaster muscle; Ref. 154). Observing erythrocyte velocity and measuring capillary length, Honig et al. (86) calculated mean transit times of 4.3 s with a range of 0.09–43 s in rat gracilis.

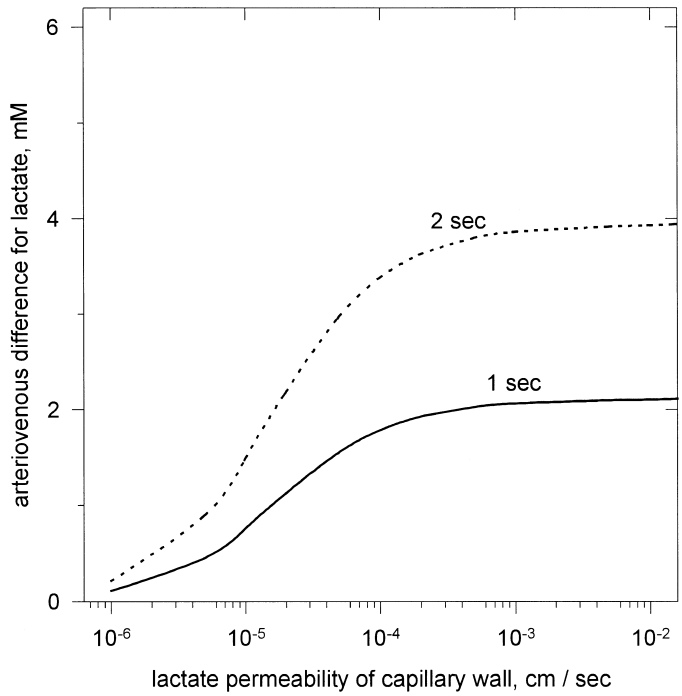

FIG. 7. Computed effect of capillary permeability for lactate on arteriovenous concentration difference of lactate. Conditions chosen for the calculation are as follows: intramuscular lactate concentration, 40 mM; arterial lactate concentration, 2 mM; P_{CO_2}, 7.3 kPa (55 mmHg). Carbonic anhydrase (CA) activity is given as the factor by which the uncatalyzed reaction is accelerated, i.e., an activity of A = 1 indicates the uncatalyzed reaction. CA activities assumed for these calculations were as follows: in erythrocytes, A = 6,500; CA associated with capillary wall expressed as activity in capillary plasma, A = 100; sarcolemmal CA expressed as activity in the interstitial space, A = 100. Dotted line, capillary transit time 2 s; solid line, capillary transit time 1 s.

It may be noted that although the value of the capillary transit time is obviously critical for the calculated arteriovenous difference for lactate (Fig. 7), this is not the case for the arteriovenous difference for CO_2. Almost no difference was calculated for CO_2 excretion using transit times between 0.5 and 2 s when no lactate excretion was present. However, when lactate excretion was present and increased with increasing transit times, as just explained, the calculated arteriovenous difference for CO_2 decreased with increasing transit times, probably due to the accompanying metabolic acidosis. It may be speculated whether long transit times are useful (and present?) in more glycolytically working muscles such as gracilis muscle, in contrast to oxidatively operating muscles, in which shorter transit times might be sufficient.

D. Effect of CA at Different Localizations on Equilibration of Intravascular pH, CO_2 Excretion, and Excretion of Lactic Acid

1. CA inside erythrocytes

It is well established that the presence of an intraerythrocytic CA is essential for an efficient transport of CO_2 by the blood. For the calculations of Figure 8, a constant P_{CO_2} in muscle cells of 7.3 kPa (55 mmHg) was assumed, and it was further assumed that CA is available to plasma by a CA bound to the endothelium with a 100-fold acceleration of the hydration velocity (A = 100). In addition, it was assumed that muscle lactate concentration is low so that there is negligible lactate excretion.

The calculations give the following results: *1*) when only uncatalyzed dehydration-hydration reaction occurs in erythrocytes (no catalysis, defined here as CA activity A = 1), a very low arteriovenous difference for total CO_2 (i.e., CO_2 + HCO_3^- + carbamate) is obtained (Fig. 8, *bottom*). The CO_2 binding capacity of the blood at the given P_{CO_2} of 7.3 kPa (55 mmHg) can only partially be used, because the velocity of the hydration reaction in erythrocytes is far too slow in comparison with the capillary transit time of 1 s. Most of the arteriovenous difference under these conditions is due to dissolved CO_2 and carbamate.

2) When the dehydration-hydration reaction velocity is 1,000-fold enhanced (CA activity A = 1,000), the arteriovenous difference for CO_2 is 98% of its maximal value, which can be achieved given the conditions indicated (Fig. 8, *bottom*). This is close to the value of A = 600 that can be estimated from Roughton (147) to be the necessary acceleration of the dehydration reaction in the lung for CO_2 exchange to achieve 98% of its maximal value within capillary transit time during rest. It is not clear why there is so much more CA activity inside erythrocytes than is apparently necessary. An increase of the intramuscular partial pressure of CO_2 to values as high as 13.3 kPa (100 mmHg) does not require any higher CA activity inside erythrocytes. The curve of Figure 8 showing the dependency of arteriovenous difference on CA activity is shifted to higher values of arteriovenous differences but does not alter its shape. The same holds for a higher HCO_3^- permeability of the erythrocyte membrane: when the HCO_3^- permeability is assumed to be three times higher than the standard value used, the arteriovenous differences are unaltered compared with those seen in Figure 8. This implies that no additional CA would be necessary if the permeability of the erythrocyte membrane for HCO_3^- were higher. (It may be noted that massive reduction of HCO_3^- permeability per se decreases CO_2 excretion in the lung, Ref. 23). In other words, neither does the HCO_3^- permeability of the red cell membrane set a limit to CO_2

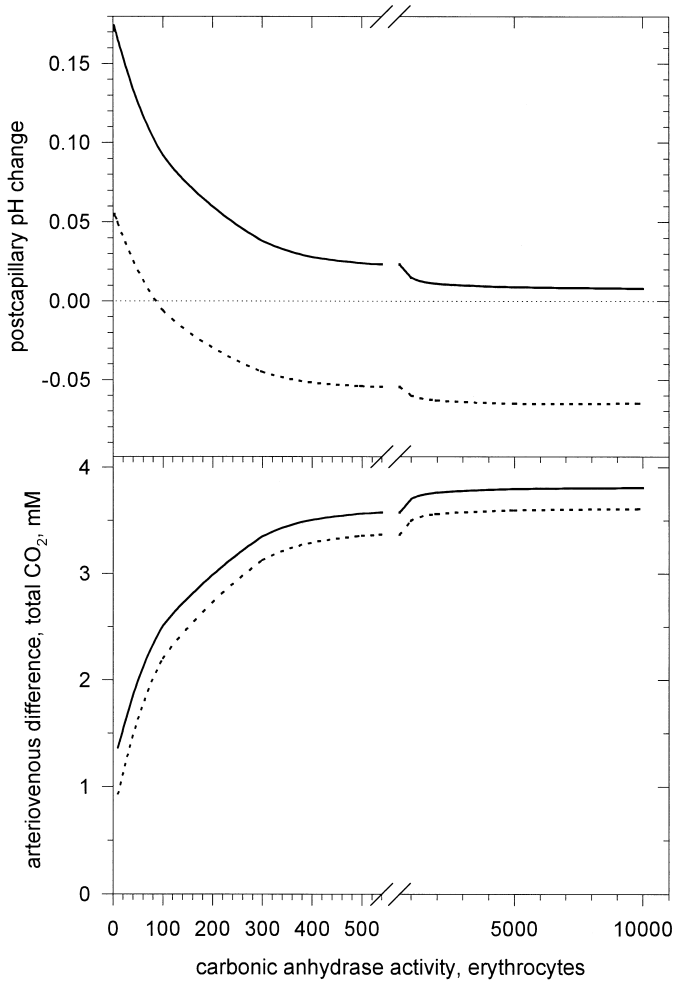

FIG. 8. Computed effect of erythrocyte carbonic anhydrase activity on postcapillary pH equilibrium and CO_2 excretion, expressed as arteriovenous difference of total CO_2. Conditions chosen for the calculation are as follows: P_{CO_2} in muscle cell, 7.3 kPa (55 mmHg); intramuscular lactate concentration, 4 mM; arterial lactate concentration, 2 mM; capillary transit time, 1 s. Solid lines: carbonic anhydrase activity (A): capillary wall, A = 100; sarcolemma, uncatalyzed A = 1. Dotted lines: CA activity: capillary wall, uncatalyzed, A = 1; sarcolemma, uncatalyzed A = 1.

uptake, nor does red cell CA activity ever become limiting at increased levels of CO_2 production. A possible situation where intraerythrocytic CA may become more critical, which has to our knowledge never been investigated, is a severe lactic acidosis with low intraerythrocytic pH values. At a pH of 6.4, the activity of CA II decreases to ~30% of its value at pH 7.2 (99), and in this situation, more enzyme will be necessary to maintain the required activity.

3) The dotted line in Figure 8, *bottom*, shows arteriovenous differences of total CO_2 in the absence of extracellular, intravascular CA activity, whereas the solid line indicates presence of A = 100 in capillary plasma volume. Lack of intravascular CA results in a decrease in arteriovenous difference by an about constant amount. This is due to the inability of the plasma to utilize its own buffer capacity during capillary transit. The reduction in CO_2 uptake amounts to only a few percent at high red cell CA activities but is relatively more important when red cell CA activity is low or absent.

4) When only uncatalyzed dehydration-hydration reaction is present in erythrocytes, there is a large and very slow postcapillary pH shift of >0.15 pH units in the plasma in alkaline direction (Fig. 8, *top*, solid line). The ΔpH values given in Figure 8, *top*, represent the maximal deviations of endcapillary plasma pH from their equilibrium values. The large pH shifts occur, although in the calculation represented by the solid line, capillary CA activity is assumed to be available to the plasma during capillary transit (A = 100). In the absence of intraerythrocytic CA activity, no full pH equilibrium was achieved even within the period of 120 s considered in our calculations. In this case, the buffer capacity of the erythrocytes, which is ~10 times greater than that of plasma, can only be used slowly, since CO_2 within erythrocytes is very slowly converted to H^+ and HCO_3^-. The slow alkaline postcapillary pH shift seen here in the plasma is essentially caused by the slowly decreasing P_{CO_2} in the whole blood, which reflects the slow formation of HCO_3^- inside the red blood cell and thus the slow formation of the major storage form of CO_2 in the blood. Accordingly, the postcapillary pH shift disappears when intraerythrocytic CA activity increases beyond A = 1,000, as shown by the solid line.

5) When no CA is available to the plasma in the capillary (dotted line in Fig. 8, *top*), the curve showing the function of postcapillary pH change versus erythrocyte CA activity is of similar shape but is shifted by ~0.1 pH unit toward more acidic postcapillary pH changes. When in this situation intraerythrocytic CA activity is low, the differences between endcapillary pH and equilibrium pH, i.e., the overall postcapillary pH changes, as given on the *y*-axis of Figure 8, are small or even absent. However, immediately after leaving the capillary, pH of the plasma falls within a few seconds to increase slowly toward the equilibrium value thereafter. A similar observation has been made in lung models (10).

6) Lactate excretion is almost independent of the presence of CA in erythrocytes, as can be expected (see below and Fig. 11).

What would be the impact of CA-deficient erythrocytes in vivo? As it is well known and as Figure 8 demonstrates, erythrocytes without CA activity can transport far less CO_2 than red blood cells with CA activity, but such a situation does not exist among vertebrates. Even the most primitive of them, e.g., agnathans, has CA activity inside their erythrocytes (see Table 4).

There are genetic disorders and there are experiments with inhibition of CA activity that allow us to study the consequences of reduced levels of CA in red blood cells. Clinical manifestations attributed to deficiency of a CA, the CA II deficiency syndrome, encompass osteopetrosis, renal tubular acidosis, and cerebral calcifications as reviewed by Sly and co-workers (162, 163). However, in the erythrocytes of these patients, there is still activity of CA I present. This isozyme occurs normally in adult human erythrocytes at a greater concentration than CA II does, but because of its higher sensitivity for Cl^-, it is inhibited to a large extent. At 37°C, it contributes ~50% of the normal activity in red blood cells (33). When in normal red blood cells the hydration reaction is accelerated by a factor of ~14,000 over the uncatalyzed rate (CA activity = 14,000), then loss of one-half of this activity (A = 7,000) cannot be expected to reduce CO_2 transport from muscle to blood even slightly (Fig. 8). The manifestations of CA II deficiency in other tissues are far more prominent clinically, and no disturbances of CO_2 elimination of the body are apparent.

There are no techniques available to perform experiments in vivo, in which erythrocytic CA activity only is inhibited, because after intravasal administration of CA inhibitors these will not only diffuse readily into the interior of erythrocytes but will always inhibit necessarily any extracellular CA activity in the lung as well as in other tissues, and will in addition penetrate into the cells of several other tissues. For example, CO_2 excretion across alveolar membrane will always be affected by such CA inhibitors. The overall effect of this systemic CA inhibition on blood gases, tissue P_{CO_2}, and ventilation has been demonstrated in classical experiments by Roughton et al. (148), Mithoefer (121), Mithoefer and Davis (122), and Swenson and Maren (166). A few experiments are available in which it was attempted to demonstrate the role of CA in CO_2 excretion by specific tissues, by either observing tissue P_{CO_2} or organ arteriovenous differences. An increase in tissue P_{CO_2} by ~1.3 kPa (10 mmHg) during the reduction of CA activity has been observed for tissue surrounding the eye, whereas venous and arterial P_{CO_2} values were not significantly changed in this experiment (169). Kowalchuk et al. (106) measured a decrease in the

arteriovenous concentration differences for HCO_3^- and CO_2 across the human forearm and thus a decrease in CO_2 excretion, during forearm exercise, after administration of acetazolamide. These effects are independent of the accompanying effect on CO_2 excretion by the lung, and these reductions in CO_2 excretion probably reflect mostly the inhibition of CA inside erythrocytes and only to a minor extent the inhibition of extracellular CA (see below). Differentiation between an effect due to red cell CA inhibition and one due to extra- or intracellular tissue CA inhibition at the moment is only possible from theoretical models such as are described in section IV, *D2* and *D3*.

For the computations described in the following, CA activity within erythrocytes was always chosen to be 6,500 for technical reasons linked to the numerical procedure. Although the actual activity within erythrocytes is reported to be higher, this acceleration is more than fast enough not to become the rate-limiting step for the processes modeled. The size of necessary time intervals for the calculation would have to become much smaller with higher speed of the hydration reaction, and this would consequently slow down the speed of the calculation and, more importantly, increase the necessary precision requirements for all values.

2. CA at the capillary wall

Carbonic anhydrase associated with endothelium provides CA activity for plasma during capillary passage. Figure 9 shows the computational results for what the presence of CA in the plasma during capillary transit does to *1*) arteriovenous difference of CO_2 and *2*) the equilibration of pH in the plasma after blood has left the capillary. The calculations were done for the following conditions: intramuscular P_{CO_2} 7.3 kPa (55 mmHg), lactate concentration in the muscle cell of 4 mM, and hydration-dehydration reaction in the interstitial space uncatalyzed.

The calculations yield the following results (Fig. 9). *1*). With the assumption of uncatalyzed velocity for the dehydration-hydration reaction inside capillary plasma, the arteriovenous difference as a measure of CO_2 excretion is ~6% less when compared with a situation when a CA activity of ~50 or more is available to the plasma (solid curve in Fig. 9, *bottom*). With a CA activity of only ~10 available to the plasma, about one-half of this increase in CO_2 excretion can be achieved. The absence of CA activity from capillary plasma can be compensated by an elevation of muscle tissue P_{CO_2}; if muscle P_{CO_2} is raised only ~0.27 kPa (2 mmHg) in this example and all other parameters remain unchanged, then the arteriovenous difference even without plasma CA activity becomes as high as it is with plasma CA present. Thus presence of CA at the capillary wall and presence of CA activity within capillary plasma has minor consequences for CO_2 excretion from muscle tissue into the blood, and this decrease in excretion can be compensated for by a slightly higher P_{CO_2} gradient from muscle cells to arterial blood.

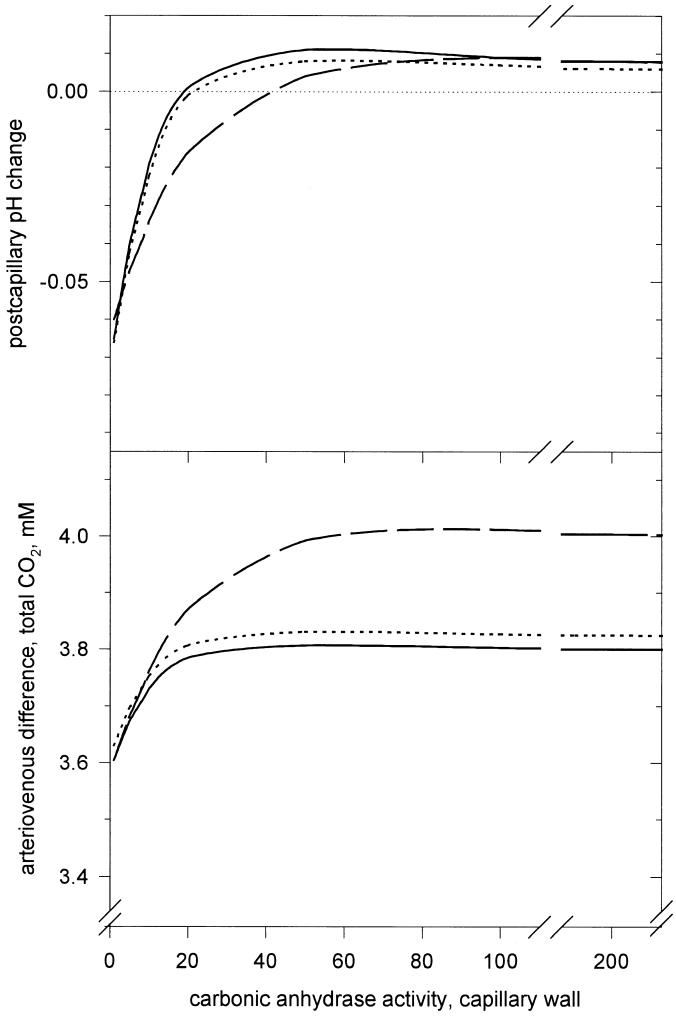

FIG. 9. Computed effect of carbonic anhydrase bound to the capillary wall and available to plasma. Conditions chosen for the calculation are the same as those in Fig. 7 with a CA activity within erythrocytes A = 6,500 and at the sarcolemma A = 1. Solid line, calculated with the normal nonbicarbonate buffer capacity of the plasma β = 5.5 mM/unit pH, as used for most of the calculations here; dashed line, calculated with a nonbicarbonate buffer capacity of plasma β = 11 mM/unit pH; dotted line, calculated under the assumption of a 3 times higher than normal bicarbonate permeability for the erythrocyte membrane; this increased bicarbonate permeability has almost no effect on arteriovenous difference for CO_2.

For a more severe respiratory acidosis, P_{CO_2} ~9.3 kPa (70 mmHg), the results are qualitatively similar, but absolute arteriovenous-differences are of course higher. However, the necessary increase in intramuscular P_{CO_2} to achieve a compensation of the decrease in arteriovenous difference when CA is not available to plasma is twice as high as in the former example. Thus the CA associated with capillary wall appears to become more important for efficient CO_2 excretion when the work load of the muscle increases.

In agreement with this, we made the following observation in an isolated blood-perfused rat hindlimb. When extracellular CA was inhibited by benzolamide and quaternary ammonium sulfonamide (QAS), inhibitors which are thought to be confined to the extracellular space and thus erythrocytic CA is left essentially uninhibited, no reduction of CO_2 excretion during rest and during moderate exercise with a fourfold increase in O_2 consumption could be detected (49). This is as is to be expected from these computational results.

Henry et al. (82), however, found in the isolated perfused white tail muscle of the trout that inhibition of extracellular CA by QAS, an inhibitor confined to the extracellular space, reduced CO_2 efflux from this muscle by ~30% and caused a significant increase in intramuscular P_{CO_2} by ~0.4 kPa (3 Torr). It may also be noted that inhibition of the membrane-associated CA IV of the isolated blood-free perfused lung reduced CO_2 excretion by this lung preparation significantly (76).

2) With respect to equilibration of postcapillary pH, however, CA associated with the capillary wall of skeletal muscle is important (Fig. 9, *top*). When no CA activity is present in plasma, there is a large pH shift in acidic direction after blood has left the capillary. The blood leaving the capillary is more alkaline than at equilibrium distribution between erythrocytes and plasma. Equilibration across erythrocytic membrane takes time, and postcapillary pH of plasma shifts slowly toward the more acid equilibrium pH. Such a time course of exchange between erythrocytes and plasma after CO_2 uptake in the absence of extracellular CA was already measured and reproduced with a theoretical model by Forster and Crandall (45). This acid postcapillary shift develops because during capillary passage H^+ are produced in large amounts inside the red blood cell but, in the absence of plasma CA, not in plasma. So H^+ have to be transferred from the red blood cell to the plasma, but this H^+ transfer is too slow to happen during capillary transit time. It occurs mainly by the Jacobs-Stewart cycle, whose rate is limited by the slow extraerythrocytic hydration-dehydration reaction velocity. When just a small amount of enzyme activity is available to the plasma, this acidic shift is abolished, as seen in Figure 9. The CA activity necessary in the plasma to achieve a half-maximal effect is ~10. With maximal CA available to plasma, there is still a very small pH shift in the alkaline direction. This alkaline shift is smaller when the HCO_3^- permeability of the erythrocyte membrane is taken to be three times higher in the calculations than the normal value.

It may be noted, but is not shown, that the alkaline shift is further increased by ~0.003 pH units in this example, when in addition to CO_2 excretion lactate excretion is present at a rate equivalent to that of CO_2. The reason for this additional slow alkaline shift is the very slow process of lactic acid equilibration between erythrocytes and plasma (Table 9), where the half-time of lactate uptake into erythrocytes even in the presence of a specific lactate-H^+ cotransporter, as it occurs in some species, is 35 s (91), but without such a transporter this time is even 6.5 min (4).

For muscle tissue perfused with saline, O'Brasky and Crandall (129) have investigated the importance of capillary CA for rapid pH equilibration in the postcapillary perfusate. In the blood-perfused hindlimb, inhibition of the extracellular CA produced postcapillary pH shifts in the acidic direction. When no inhibitors of CA were present, the postcapillary pH shift was not abolished, but instead an alkaline pH shift was observed (49).

3) For lactate excretion, our model predicts that capillary CA, i.e., CA in capillary plasma, has no effect whatsoever.

The dashed curves in Figure 9 show the effect of a plasma nonbicarbonate buffer capacity that is doubled from its normal value of 5.5 to 11 mM/ΔpH. As can be expected, this leads to an increase in CO_2 arteriovenous difference (and CO_2 excretion) by ~5%, and more intracapillary CA activity is required to utilize this increased plasma CO_2 binding capacity. Similarly, the acid postcapillary pH shift requires more intravascular CA activity under this condition to fall toward zero. This again implies that more CO_2 has to be hydrated in the plasma to produce the pH required for equilibrium, when plasma buffer capacity is higher. In conclusion, capillary CA activity becomes more important with increasing plasma buffer capacity.

These computational results remain essentially unchanged with the assumption of the additional presence of CA activity associated with the sarcolemma, or interstitial CA activity. Carbon dioxide excretion and change of postcapillary pH are the same as without interstitial CA activity.

In conclusion, intravascular CA activity is of some relevance for CO_2 excretion, which depends on plasma buffer capacity, but interstitial CA does not contribute to this process and instead serves entirely another purpose, as shown section IV*D3*.

3. CA associated with the sarcolemma

Carbonic anhydrase associated with the sarcolemma is with its active center oriented toward the extracellular space and thus provides acceleration of the hydration-dehydration reaction on the muscle cell surface and in the interstitial space. Bicarbonate is therefore expected to be a potent and rapidly available buffer in this compartment, which possesses a very low nonbicarbonate buffer capacity. Juel (94) has shown that the external buffer capacity around sarcolemmal vesicles can affect lactate efflux.

Conditions chosen for the following computations were high concentrations in the muscle of both CO_2 (P_{CO_2}

55 mmHg) and lactate (40 mM in the muscle cell). In addition to an intraerythrocytic CA activity of 6,500, an intracapillary CA activity of 100 was used. Computational results were as follows.

1) When no CA is present at the sarcolemma, the interstitial pH becomes rather low (Fig. 10, *top*, dotted line), indicating that interstitial HCO_3^- does not react fast enough to buffer the H^+ of the lactic acid leaving the muscle cells. Only a very small acceleration of the dehydration rate within the interstitial space is sufficient to keep the interstitial pH close to 7.15. Under these conditions, a CA activity of only ~5 achieves a half-maximal effect. However, when almost no lactate is excreted by the muscle cell (arteriovenous lactate concentration difference ~0.6 mM), CA at the sarcolemma becomes rather unimportant for the pH equilibrium in the interstitial space (Fig. 10, *top*, solid line).

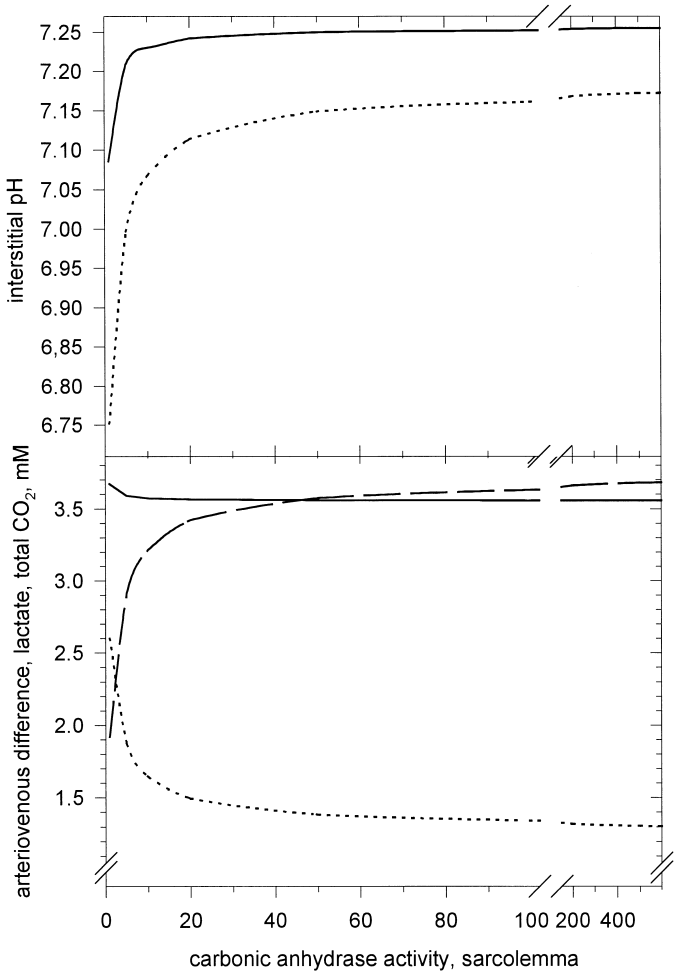

FIG. 10. Computed effect of carbonic anhydrase associated with the sarcolemma, i.e., carbonic anhydrase activity within the interstitial space, on interstitial pH, and arteriovenous concentration differences of lactate and total CO_2. Conditions chosen for the calculation were as follows: intramuscular P_{CO_2}, 7.3 kPa (55 mmHg); carbonic anhydrase activities: in erythrocytes A = 6,500, in capillary A = 100; transit time, 2 s. All solid lines, intramuscular lactate concentration 40 mM and arterial lactate concentration 2 mM; all dashed or dotted lines, intramuscular lactate concentration 4 mM and arterial lactate concentration 2 mM. In *bottom panel*, dashed line, arteriovenous difference for lactate; solid and dotted lines, arteriovenous difference for total CO_2.

2) Plasma postcapillary pH changes were not influenced by presence or absence of sarcolemmal CA activity (data not shown); here intravascular CA activity, together with intraerythrocytic activity, alone is crucial.

3) When CA at the sarcolemmal surface is lacking, the arteriovenous difference for lactate is reduced to almost by one-half (Fig. 10, *bottom*, dashed line). As discussed above, this can be expected to occur as a consequence of the decrease in interstitial pH, which slows down lactic acid excretion via lactate-H^+ cotransport. A fivefold acceleration of the hydration-dehydration rate in the interstitial space is sufficient to produce a half-maximal increase in lactate excretion.

Experimentally, such an effect of CA on lactate excretion has been observed. In a blood-perfused rat hindlimb preparation, selective inhibition of extracellular CA reduced lactate excretion significantly (49). In these experiments, CA activity of the capillary wall as well as that associated with the sarcolemma were inhibited. From the experiments, therefore, it could not be decided which CA at which location is responsible for the reduction of lactate release. From the present theoretical model, we conclude that inhibition of the sarcolemmal CA only is responsible. This conclusion presumably holds also for the observations of Kowalchuk et al. (106), who reported a decreased lactate release into the blood under systemic treatment with acetazolamide.

Carbon dioxide release in Figure 10, *bottom*, dotted line, appears to be impaired with increasing activity of sarcolemmal CA, yet CO_2 release per se is not dependent on CA in this location. When no significant lactate excretion occurs, there is no change in CO_2 excretion whatsoever associated with a change in sarcolemmal CA activity (Fig. 10, *bottom*, solid line). However, as the difference between solid and dotted lines in Figure 10, *bottom*, suggests, the arteriovenous difference for total CO_2 is higher when no or little lactate excretion occurs than when major lactate excretion is present. It is the increase in lactate excretion caused by an increase of sarcolemmal CA activity, which reduces total CO_2 excretion from the muscle, when sarcolemmal CA activity increases along the abscissa in Figure 10. The reason for this is as follows: when CA activity is present in the interstitial space, a higher rate of lactate-H^+ cotransport out of the muscle cell takes place. More H^+ arrive in the blood, and pH in plasma and in red blood cells decreases. This implies that, at a given P_{CO_2} (here 55 mmHg), the total CO_2 bound in the blood is reduced, because both HCO_3^- and carbamate decrease with decreasing pH. Thus lactic acidosis decreases the total CO_2 release from muscle into blood at a given P_{CO_2}. Because CO_2 production continues, the consequence is

a rise in tissue and venous blood P_{CO_2} values. For the whole body, heavy exercise therefore is associated with rather high muscle venous P_{CO_2} values and, as is well known, part of this CO_2 is mobilized by lactic acid from the CO_2 stores in muscle and blood.

The major conclusion from the results presented in Figure 10 then is that sarcolemmal CA plays an important role in the *1*) maintenance of normal interstitial pH by making the interstitial HCO_3^- rapidly available buffering of H^+ of fixed acids, and, linked to this, *2*) facilitation of lactic acid release from the muscle cell by consuming the H^+ leaving the cell along with lactate. In contrast, sarcolemmal or interstitial CA does not appear to be involved in the exchange of CO_2 in skeletal muscle.

4. Lactic acid excretion and CA

The role of the three types of CA considered here for the excretion of lactic acid from muscle is summarized in Figure 11. It is immediately apparent from Figure 11 that only interstitial, sarcolemmal CA plays a major role. Lack of this enzyme slows down lactic acid release from muscle cells by the mechanism just discussed, which results in a diminished arteriovenous difference of lactate in the blood.

Carbonic anhydrase activity inside the red blood cell is of minor importance but does have a small effect (dotted curve in Fig. 11). The cause underlying this effect is that in the presence of CA in erythrocytes, more HCO_3^- and H^+ are produced within red blood cells from CO_2 taken up. The H^+ are buffered by hemoglobin, and part of the HCO_3^- is released from the erythrocytes into the plasma. Accordingly, the pH of plasma within the capillary and also the pH of the interstitial space are slightly more alkaline (calculated under these conditions by 0.04 and 0.03 units, respectively) than in the absence of CA in erythrocytes. The more alkaline pH of the interstitial space enhances lactate-H^+ cotransport and thus increases the arteriovenous difference of lactate.

Carbonic anhydrase activity in the capillary plasma has no apparent effect on lactate release at all (dashed curve in Fig. 11).

Thus the CA isozyme relevant for lactic acid excretion is almost exclusively the sarcolemmal extracellular CA.

It may be noted that the effect of interstitial CA on lactate release seen in Figure 11 critically depends on the pH dependence of the H^+-lactate cotransporter and will increase when the pH dependence is greater than assumed here. More importantly, the calculation of Figure 11 is valid only under steady-state conditions, and the role of sarcolemmal CA for lactic acid release is expected to become much greater under non-steady-state conditions. Kowalchuk et al. (106) have indeed made their observations on the inhibitory effect of acetazolamide on lactate uptake by the blood in a non-steady-state situation, immediately after a 30-s period of maximal exercise.

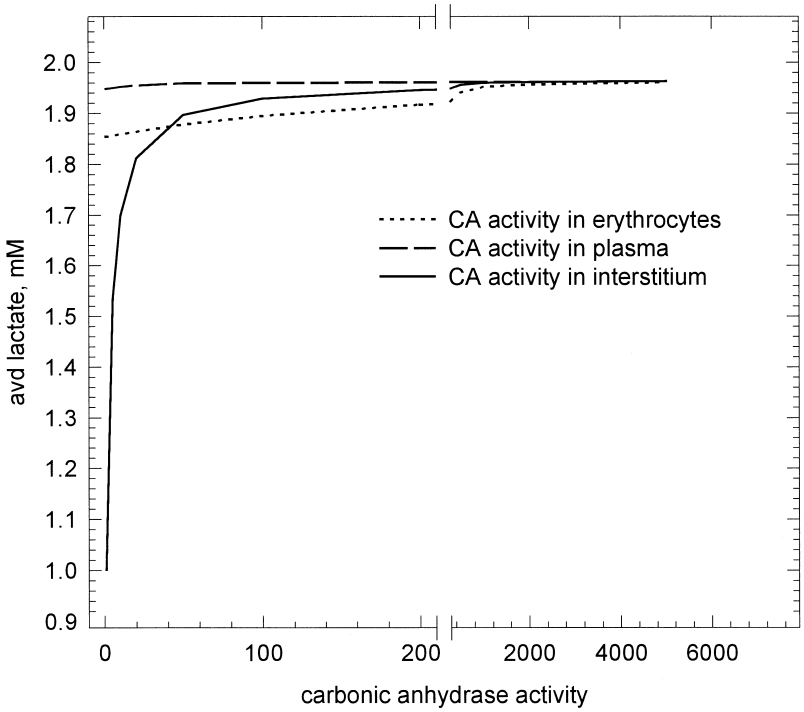

FIG. 11. Effect of carbonic anhydrase (CA) activity in erythrocytes, capillary plasma, or interstitium, respectively, on arteriovenous concentration difference of lactate (avd). CA activity was varied in one compartment, while the activity in the two other compartments was high enough to be not limiting (CA in erythrocytes, A = 10,000; CA in capillary, A = 1,000; CA on sarcolemma, A = 1,000). Conditions chosen for the calculation were as follows: intramuscular P_{CO_2}, 7.3 kPa (55 mmHg); intramuscular lactate concentration, 40 mM; arterial lactate concentration, 2 mM. It can be concluded from the figure that it is essentially only the sarcolemmal, interstitial CA that affects lactate release from muscle.

5. Possible physiological role of the plasma inhibitor of CA

The plasma inhibitor makes sure that any activity of CA released from hemolysed erythrocytes is suppressed in the plasma. The physiological role of this plasma inhibitor of CA, which is found in several species, is not known.

One attempt at an explanation could be that a rapid pH equilibration of the blood within the capillary, as it is achieved by the presence of CA in the capillary plasma, is not useful in some species for the following reason. When pH equilibrium is not achieved in the capillary and all the H^+ formed are still inside the red blood cells (with the consequence of a slow acid postcapillary pH shift), then a maximum Bohr effect of hemoglobin is achieved and a maximum of O_2 should be released from the red blood cells during capillary transit. This may be generally useful to maximize O_2 supply to the tissue and may be particularly important in fishes that require high rates of O_2 secretion in the swim bladder or the rete mirabile of the eyes. The plasma inhibitor according to this idea would inhibit plasma CA and optimize O_2 unloading in all tissues that do not have an intracapillary CA. Tissues that require optimization of their CO_2 elimination rather than their O_2 supply may then be equipped with an intracapillary CA, making this enzyme available in that organ only.

This prompted us to calculate what effect the presence of CA activity in the capillary plasma has on intracellular pH of erythrocytes within the capillary. Figure 12 shows that in principle this effect does indeed occur; in the absence of capillary CA, endcapillary pH of the intraerythrocytic cytoplasm is ~0.02 units lower than in the presence of a capillary CA activity of 20 or more. These calculations were performed for conditions of a high intramuscular P_{CO_2} (~8 kPa; 60 mmHg) and high lactate concentration (40 mM), but also with a low lactate excretion and with a P_{CO_2} of ~7.3 kPa (55 mmHg), the result is qualitatively similar. Thus plasma inhibitor of CA in principle contributes to tissue oxygenation by decreasing intraerythrocytic pH beyond its equilibrium value during capillary passage. This decrease in pH will increase the Bohr effect. However, as is apparent from Figure 12, the effect calculated here is rather small and will improve O_2 unloading very little. It thus appears unlikely that this is a major physiological purpose of the plasma inhibitor.

Another possible function of a plasma CA inhibitor emanates from the studies of Wood and Munger (186) on the effect of CA injection into the circulation on the stimulation of ventilation after exhaustive exercise in rainbow trout. These authors found that CA added to the plasma caused a very significant increase in arterial pH and decrease in arterial P_{CO_2} at rest and more so after exhaustive exercise. In the postexercise period, elevated arterial pH and decreased arterial P_{CO_2} resulted in a reduced postexercise hyperventilation, decreased postexercise O_2 uptake, and decreased arterial P_{CO_2}. Thus, in the postexercise situation, CO_2 release appeared to be optimized by plasma CA, but this occurred at the expense of decreased ventilatory drive and decreased O_2 supply. Thus, under the aspect of the ventilatory drive exerted by P_{CO_2}, it may be useful to suppress any plasma CA in the circulatory system by a plasma inhibitor. It would be desirable to do experiments analogous to those of Wood and Munger (186) in a mammalian system.

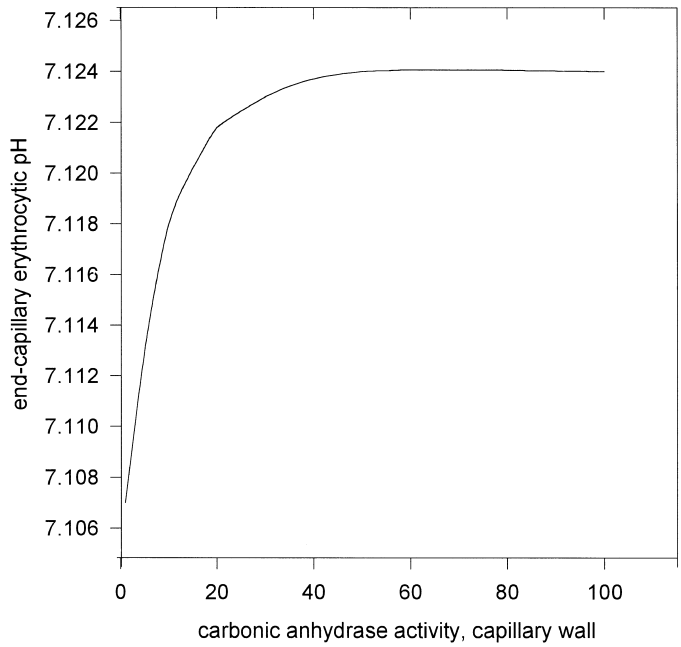

FIG. 12. Computed effect of capillary carbonic anhydrase available to capillary plasma, or effect of plasma inhibitor, respectively, on intraerythrocytic pH at the end of the capillary. Conditions chosen for the calculation were as follows: intramuscular lactate concentration, 40 mM; arterial lactate concentration, 2 mM; carbonic anhydrase activities: in erythrocytes, A = 6,500; on sarcolemma, A = 100. A constant arteriovenous difference for total CO_2 of 4.00 mM is achieved by slightly varying intramuscular P_{CO_2} between 8.23 and 8.56 kPa (61.9–64.4 mmHg); when less carbonic anhydrase activity is present in the capillary plasma, the intramuscular P_{CO_2} has been set higher to keep CO_2 excretion constant. It can be concluded from the figure that absence of capillary carbonic anhydrase causes a more pronounced intraerythrocytic acidification at the end of the capillary, thus producing a maximal Bohr effect.

V. APPENDIX

This appendix illustrates the equations used for the mathematical model.

A. Interstitial Concentrations of CO_2, HCO_3^-, H^+, and Lactate

The transit time necessary for the blood to travel through a capillary is divided into small time steps. During

each time step, blood faces a small part of the interstitial space. For steady-state conditions, interstitial concentrations of lactate, HCO_3^-, CO_2, and H^+ were assumed to be stable within this small part. Thus, for one species, the sum of all changes within the interstital space, i.e., influx and efflux into this space and in the case of CO_2, HCO_3^-, and H^+ its forward and backward reaction, has to be zero. For each time step of the blood, the four unknown interstitial concentrations in the small part of the interstitial space are calculated using four equations (*Eqs. A1—A4*). Concentrations of plasma were taken from the preceding time step, and muscle concentrations were assumed to be constant. Thus a concentration profile for the interstitial space along the capillary is calculated.

For CO_2

$$0 = ([CO_2]_{sm} - [CO_2]_i) \times \frac{P_{CO_2} \times A_{SL}}{vol_i \times 1{,}000} - ([CO_2]_i - [CO_2]_p) \times \frac{P_{CO_2} \times A_{Kap}}{vol_i} - CA_i \times \left(k_{CO_2} \times [CO_2]_i - k_{H_2CO_3} \times \frac{[H^+]_i \times [HCO_3^-]_i}{K_1}\right) \quad (A1)$$

For HCO_3^-

$$0 = CA_i \times \left(k_{CO_2} \times [CO_2]_i - k_{H_2CO_3} \times \frac{[H^+]_i \times [HCO_3^-]_i}{K_1}\right) - ([HCO_3^-]_i - [HCO_3^-]_p) \times \frac{P_{HCO_3^-} \times A_{Kap}}{vol_i} \quad (A2)$$

For H^+

Lactate and H^+ are transported equimolar across the sarcolemma; thus for H^+ flux across this membrane, the same term is used for lactate and H^+. H^+ transport out of the muscle cell by other transporters is neglected.

$$0 = \left(\frac{[La^-]_{sm} \times V_{max}}{K_m + [La^-]_{sm}} - \frac{[La^-]_i \times V_{maxR}}{K_m + [La^-]_i}\right) \times \frac{A_{SL}}{vol_i} + CA_i \times \left(k_{CO_2} \times [CO_2]_i - k_{H_2CO_3} \times \frac{[H^+]_i \times [HCO_3^-]_i}{K_1}\right) - ([H^+]_i - [H^+]_p) \times \frac{P_{H^+} \times A_{Kap}}{vol_i} \quad (A3)$$

For lactate

$$0 = \left(\frac{[La^-]_{sm} \times V_{max}}{K_m + [La^-]_{sm}} - \frac{[La^-]_i \times V_{maxR}}{K_m + [La^-]_i}\right) \times \frac{A_{SL}}{vol_i} - ([La^-]_i - [La^-]_p) \times \frac{P_{La^-} \times A_{Kap}}{vol_i} \quad (A4)$$

Dependence of H^+-lactate cotransport on pH was assumed to be linear for the relevant pH range. With a decrease of pH from 7.4 by one unit, lactate flux decreases to a fraction (Vr) of the flux at pH 7.4 (calculated as in Ref. 93)

$$V_{max} = V_{max,7.4} \times \{1 - Vr(7.4 + \log_{10}[H^+]_i - 3)\}$$

$$V_{maxR} = V_{max,7.4} \times [1 - Vr(7.4 - pH_{sm})]$$

B. Concentration Changes Within Plasma and Erythrocytes

Concentration changes are calculated for erythrocytes and plasma as blood flows along the capillary wall using the interstitial concentration as calculated above for each time step.

1. *CO₂*

$$\frac{d[CO_2]_e}{dt} = \left(-k_{CO_2} \times [CO_2]_e + k_{H_2CO_3} \times \frac{[H^+]_e \times [HCO_3^-]_e}{K_1}\right) \times CA_e - \frac{d[carb]}{dt} + ([CO_2]_p - [CO_2]_e) \times \frac{P_{CO_2} \times A_e}{wvol_e}$$

$$\frac{d[CO_2]_p}{dt} = \left(-k_{CO_2} \times [CO_2]_p + k_{H_2CO_3} \times \frac{[H^+]_p \times [HCO_3^-]_p}{K_1}\right) \times CA_p + ([CO_2]_i - [CO_2]_p) \times \frac{P_{CO_2} \times A_{Kap}}{vol_p} - ([CO_2]_p - [CO_2]_e) \times \frac{P_{CO_2} \times A_e}{vol_p}$$

2. *Carbamate*

With the assumption of constant blood flow, no anoxic regions, and constant O_2 consumption within muscle tissue along the capillary, it follows that O_2 flow across the capillary wall should be constant for each part of the capillary. Thus deoxygenation of hemoglobin during capillary passage was assumed to increase linearly along the capillary.

$$[Hb] = [Hb]_0 + \frac{t}{TZ} \times ([Hb]_{end} - [Hb]_0)$$

The actual carbamate concentration converges during each time step toward an equilibrium concentration determined by the actual concentration of CO_2, pH and actual saturation of hemoglobin with a half-time $t_{1/2}$.

$$\frac{d[carb]}{dt} = \frac{\ln 2}{t_{1/2}} \times ([Hb]_{oxy} \times zo + [Hb] \times zr - [Carb]_{alt})$$

$$z_0 = \frac{2 \times [CO_2]_e}{4 \times \left([CO_2]_e + \frac{[H^+]_e}{K_{c,oxy}} + \frac{[H^+]_e^2}{K_{c,oxy} \times K_{z,oxy}}\right)}$$

$$z_r = \frac{2 \times [CO_2]_e}{4} \times \left(\frac{1}{[CO_2]_e + \frac{[H^+]_e}{K_{c,\alpha}} + \frac{[H^+]_e^2}{K_{c,\alpha} \times K_{z,\alpha}}} + \frac{1}{[CO_2]_e + \frac{[H^+]_e}{K_{c,\beta}} + \frac{[H^+]_e^2}{K_{c,\beta} \times K_{z,\beta}}}\right)$$

3. HCO_3^-

$$\frac{d[HCO_3^-]_p}{dt} = \left(k_{CO_2} \times [CO_2]_p - k_{H_2CO_3} \times \frac{[H^+]_p \times [HCO_3^-]_p}{K_1}\right) \times CA_p - \frac{\Phi_{HCO_3^-}}{vol_p} + ([HCO_3^-]_i - [HCO_3^-]_p) \times \frac{P_{HCO_3^-} \times A_{Kap}}{vol_p}$$

$$\frac{d[HCO_3^-]_e}{dt} = \left(k_{CO_2} \times [CO_2]_e - k_{H_2CO_3} \times \frac{[H^+]_e \times [HCO_3^-]_e}{K_1}\right) \times CA_e + \frac{\Phi_{HCO_3^-}}{wvol_e}$$

Φ represents anion flux from plasma to red blood cell. The equation given by Bidani et al. (10) in their theoretical model was used for HCO_3^-, and Cl^- and lactate ions were treated analogously.

$$\Phi_{HCO_3^-} = \frac{u_{HCO_3^-} \times E \times A_e}{d_e} \times \left[\frac{[HCO_3^-]_p - [HCO_3^-]_e \times e^{[-E \times F/(R \times T)]}}{1 - e^{[-E \times F/(R \times T)]}}\right] \times (mmol \cdot l^{-1} \cdot s^{-1})$$

$$\frac{d[Cl^-]_p}{dt} = -\frac{\Phi_{Cl^-}}{vol_p} \quad \text{and} \quad \frac{d[Cl^-]_e}{dt} = \frac{\Phi_{Cl^-}}{wvol_e}$$

For the initial conditions, plasma concentration of ions was given and a Donnan distribution across erythrocytic membrane was assumed.

$$\frac{[anion]_p}{[anion]_e} = e^{[E \times F/(R \times T)]}$$

3. Membrane potential

$$E = -\frac{R \times T}{F} \times \ln \frac{u_{Cl^-} \times [Cl^-]_p + u_{HCO_3^-} \times [HCO_3^-]_p + u_{La^-} \times [La^-]_p + u_{cation} \times [cation]_e}{u_{Cl^-} \times [Cl^-]_e + u_{HCO_3^-} \times [HCO_3^-]_e + u_{La^-} \times [La^-]_e + u_{cation} \times [cation]_p}$$

$u_{cation} \times [cation]$ was assumed to be 1×10^{-13} (mM·cm^2)/(mV·s), which is very low compared with the anions and serves to take a very small contribution of cations into account.

4. H^+

$$\frac{d[H^+]_p}{dt} = \frac{\ln 10 \times [H^+]_p}{\beta_p} \times \left\{\left(k_{CO_2} \times [CO_2]_p - k_{H_2CO_3} \times \frac{[H^+]_p \times [HCO_3^-]_p}{K_1}\right) \times CA_p + \left(\frac{d[H^+]_{LA_p}}{dt}\right) + ([H^+]_i - [H^+]_p) \times \frac{P_{H^+} \times A_{Kap}}{vol_p}\right\}$$

$$\frac{d[H^+]_e}{dt} = \frac{\ln 10 \times [H^+]_e}{\beta_e} \times \left\{\left(k_{CO_2} \times [CO_2]_e - k_{H_2CO_3} \times \frac{[H^+]_e \times [HCO_3^-]_e}{K_1}\right) \times CA_e + \left(\frac{d[carb]}{dt}\right) \times \gamma + \left(\frac{d[H^+]_{LA_e}}{dt}\right) - \left(\frac{d[Hb]}{dt}\right) \times \vartheta\right\}$$

Because the flux of H^+ between the plasma and erythrocyte is assumed to be very small, it was ignored here.

5. Lactate, lactic acid, and lactic acid contribution to H^+

Step 1 is change of lactate ion concentration and lactic acid concentration

$$\frac{\Delta[La^-]_p}{dt} = -\frac{\Phi_{La^-}}{vol_p} + ([La^-]_i - [La^-]_p) \times P_{La^-} \times \frac{A_{Kap}}{vol_p}$$

$$\frac{\Delta[La^-]_e}{dt} = +\frac{\Phi_{La^-}}{wvol_e}$$

H^+/La^- cotransport and nonionic diffusion were regarded together as change in lactic acid (HLa) concentration

$$\frac{\Delta[HLa]_e}{dt} = ([HLa]_p - [HLa]_e) \times P_{HLa} \times \frac{A_e}{wvol_e} + \left(\frac{[La^-]_p \times V_{max,e}}{K_{m,e} + [La^-]_p} - \frac{[La^-]_e \times V_{maxR,e}}{K_{m,e} + [La^-]_e}\right) \times \frac{A_e \times 1{,}000}{wvol_e}$$

$$\frac{\Delta[HLa]_p}{dt} = -([HLa]_p - [HLa]_e) \times P_{HLa} \times \frac{A_e}{vol_p} + ([HLa]_i - [HLa]_p) \times P_{La^-} \times \frac{A_{Kap}}{vol_p} - \left(\frac{[La^-]_p \times V_{max,e}}{K_{m,e} + [La^-]_p} - \frac{[La^-]_e \times V_{maxR,e}}{K_{m,e} + [La^-]_e}\right) \times \frac{A_e \times 1{,}000}{vol_p}$$

Step 2 is equilibration between lactic acid and lactate. After this change in the concentration of lactate ions and lactic acid during the small time step $dt = \Delta t$ (<1 ms), an equilibrium between these forms is immediately achieved. As a result, dissociation of lactic acid will increase equimolarly and simultaneously the concentration in lactate and H^+.

$$[H^+] \times [La^-] = K_{lactic\ acid} \times [HLa]$$

Taking derivatives on both sides gives

$$\frac{d[H^+]_{La}}{dt} \times [La^-] + [H^+] \times \frac{d[La^-]}{dt} = K_{lactic\ acid} \times \frac{d[HLa]}{dt}$$

With substituting in this equation

$$\frac{d[HLa]}{dt} = \frac{\Delta[HLa]}{dt} - \frac{d[H^+]_{La}}{dt} \quad \text{and}$$

$$\frac{d[La^-]}{dt} = \frac{\Delta[La^-]}{dt} + \frac{d[H^+]_{La}}{dt}$$

and solving for $d[H^+]_{La}/dt$, this gives

$$\frac{d[H^+]_{La}}{dt} = \frac{K_{lactic\ acid} \times \frac{\Delta[HLa]}{dt} - [H^+] \times \frac{\Delta[La^-]}{dt}}{[La^-] + [H^+] + K_{lactic\ acid}}$$

For plasma and erythrocytes, the appropriate indexes are to be used.

C. Volumes

$$\text{volumes:} \quad \text{whole blood} = 1 = vol_p + 0.72 \times vol_e + 0.28 \times vol_e$$

$$wvol_e = vol_e \times 0.72$$

$$\text{interstitial space, } vol_i = 2$$

Flux of water is described only across the erythrocytic membrane using a hydraulic permeability coefficient and the difference in osmolarity using the equations by Bidani et al. (10), and thus changes of volume are calculated for red blood cells and plasma only.

$$\frac{dwvol_e}{dt} = L_p \times (osm_e - osm_p) \times A_e \times V_W\ (s^{-1})$$

$$wvol_{e,neu} = \Delta t \times \frac{dwvol_e}{dt} + wvol_{e,alt}$$

$$vol_{p,neu} = 1 - wvol_{e,neu} - 0{,}28 \times vol_e = -\Delta t \times \frac{dwvol_e}{dt} + vol_{s,alt}$$

After calculations for each time step were finished, concentrations in erythrocytes and plasma were multiplied with dilution factors.

$$VF_e = \frac{wvol_{e,alt}}{wvol_{e,neu}} = \frac{wvol_{e,alt}}{wvol_{e,alt} + \Delta t \times \frac{dwvol_e}{dt}}$$

$$VF_p = \frac{vol_{p,alt}}{vol_{p,neu}} = \frac{vol_{p,alt}}{vol_{p,alt} - \Delta t \times \frac{dwvol_e}{dt}}$$

D. Solutions

The changes in erythrocytic and plasma concentrations during capillary transit were observed solving all

equations numerically for small time steps (usually 0.75 ms) after calculating for each time step the concentrations in the respective small part of the intersitial space. For postcapillary conditions, equations concerning movement out of muscle and interstitial space were removed and time steps were longer.

The programs were written in C (Borland, Vs 3.1) on a personal computer with the help of Dr. Reinhard Knörr, Institute of Mathematics, University of Rostock, Rostock, Germany.

E. Indexes Used

alt in the preceeding time step
e erythrocyte
i interstitial space
Kap capillary wall
neu in the actual time step
p plasma
SL sarcolemma
sm skeletal muscle cell

F. Abbreviations and Values of Parameters Used

A_e (7,800 cm^2/cm^3 blood) surface of erythrocytes/ml blood

A_{Kap} (5,700 cm^2/cm^3 Blut) surface capillary wall/ml blood

A_{SL} (2.85×10^7 cm^2/l blood) surface of sarcolemma/liter blood (=5 times A_{Kap})

CA (varied) carbonic anhydrase activity, factor by which the uncatalyzed reaction is accelerated

[Carb] carbamate concentration

d_e (10^{-6} cm) thickness of erythrocyte membrane

E (−9 mV) membrane potential of erythrocytes

F (96,480 C/mol) Faraday constant

[Hb] actual concentration of deoxygenated hemoglobin

$[Hb]_{end}$ concentration of deoxygenated hemoglobin in venous blood

$[Hb]_o$ concentration of deoxygenated hemoglobin in arterial blood

$[Hb]_{oxy}$ actual concentration of oxygenated hemoglobin

[HLa] lactic acid concentration

K_m (23.7 mM) H^+-lactate cotransport, skeletal muscle of rats (91)

$K_{m,e}$ (15 mM) H^+-lactate cotransport, estimate for erythrocytes (138)

k_{CO_2} (0.13 s^{-1}) CO_2 hydration velocity constant (taken from Ref. 10)

$k_{H_2CO_3}$ (57.5 s^{-1}) H_2CO_3 dehydraton velocity constant (taken from Ref. 10)

K_1 (0.35 mM) acid dissociation constant for H_2CO_3 (taken from Ref. 10)

$K_{lactic\ acid}$ ($10^{-0.86}$ mM) equilibrium constant for lactic acid

$K_{c,oxy}$, $K_{z,oxy}$, $K_{c,\alpha}$, $K_{z,\alpha}$, $K_{c,\beta}$, $K_{z,\beta}$ binding constants for carbamate (see sect. II*A*)

L_p (0.041 cm/s) bovine red cell hydraulic coefficient (taken from Ref. 10)

osm osmolarity

P_{CO_2} (1 cm/s) permeability of membranes for CO_2

P_{HLa} 3.7×10^{-5} cm/s lactic acid permeability, erythrocytes 30°C (27)

$P_{HCO_3^-}$, P_{H^+}, P_{La^-} (varied) permeability of capillary wall

R (8,314 $mJ \cdot K^{-1} \cdot mol^{-1}$) universal gas constant

T (310°K) temperature, 310°K (=37°C)

TZ (varied) capillary transit time

$t_{1/2}$ (0.12 s) for carbamate reaction (102)

t actual time after blood has entered the capillary

u_{Cl^-}, $u_{HCO_3^-}$ (2×10^{-11} $cm^2 \cdot s^{-1} \cdot mV^{-1}$) ion mobility (calculated from $P_{HCO_3^-} = 5.6 \times 10^{-4}$ cm/s; Ref. 160)

u_{La^-} (2×10^{-15} $cm^2 \cdot s^{-1} \cdot mV^{-1}$) ion mobility for lactate, estimated to be 10,000 lower than $u_{HCO_3^-}$

vol (volume/volume blood) volume of interstitial space, volume of plasma, volume of erythrocytes

$V_{max,7.4}$ (160×10^{-9} $mmol \cdot cm^{-2} \cdot s^{-1}$) maximal lactate flux in sarcolemmal vesicles; estimate for 37°C (from Ref. 91)

$V_{max,e}$, $V_{MaxR,e}$ (2.5×10^{-9} $mmol \cdot cm^{-2} \cdot s^{-1}$) maximal lactate flux in erythrocytes (estimate from Ref. 138)

V_r (0.2) fraction to which lactate flux is reduced with pH decrease from 7.4 to 6.4 (estimated from Ref. 93)

V_w (1.809×10^{-5} l/mM) millimolar volume of water (37°C)

$wvol_e$ ($0.72 \times vol_e$) volume of water within erythrocytes

zo CO_2 bound per tetramer oxygenated hemoglobin

zr CO_2 bound per tetramer deoxygenated hemoglobin

α [0.0318 mM/(1 × Torr)] solubility coefficient for CO_2

β_p (5.5 mmol H^+/unit pH) nonbicarbonate buffer capacity of plasma ($\beta_i = 0.5\beta_p$)

β_e (60 mmol H^+/unit pH) nonbicarbonate buffer capacity of erythrocytes

ϑ (0.7 mmol H^+ bound/mmol Hb_{O_2} formed) per Hb monomer (taken from Ref. 10)

Φ anion flux from plasma into erythrocytes

γ (1.8 mmol H^+ released/mmol Carb formed) (taken from Ref. 10)

Address for reprint requests and other correspondence: C. Geers, Zentrum Physiologie, Medizinische Hochschule, PO Box 61 01 80, 30623 Hannover, Germany (E-mail: Gros.Gerolf@MH-Hannover.de).

REFERENCES

1. AICKIN, C. C. Intracellular pH regulation by vertebrate muscle. *Annu. Rev. Physiol.* 48: 349–361, 1986.
2. AICKIN, C. C., AND R. C. THOMAS. An investigation of the ionic mechanism of intracellular pH regulation in mouse soleus fibres. *J. Physiol. (Lond.)* 273: 295–316, 1977.
3. AL-BALDAWI, N. F., AND R. F. ABERCROMBIE. Cytoplasmic hydrogen ion diffusion coefficient. *Biophys. J.* 61: 1470–1479, 1992.
4. AUBERT, L., AND R. MOTAIS. Molecular features of organic anion permeability in ox red blood cell. *J. Physiol. (Lond.)* 246: 159–179, 1975.
5. BALBONI, E., AND A. L. LEHNINGER. Entry and exit pathways of CO_2 in rat liver mitochondria respiring in a bicarbonate buffer system. *J. Biol. Chem.* 261: 3563–3570, 1986.
6. BANGSBO, J., L. JOHANSEN, T. GRAHAM, AND B. SALTIN. Lactate and H^+ effluxes from human skeletal muscles during intense, dynamic exercise. *J. Physiol. (Lond.)* 462: 115–133, 1993.
7. BARTELS, H., E. BÜCHERL, C. W. HERTZ, G. RODEWALD, AND M. SCHWAB. *Lungenfunktionsprüfungen.* Berlin: Springer-Verlag, 1959.
8. BAUER, C., AND E. SCHRÖDER. Carbamino compounds of haemoglobin in human adult and foetal blood. *J. Physiol. (Lond.)* 227: 457–471, 1972.
9. BIDANI, A., AND E. D. CRANDALL. Velocity of CO_2 exchanges in the lungs. *Annu. Rev. Physiol.* 50: 639–652, 1988.
10. BIDANI, A., E. D. CRANDALL, AND R. E. FORSTER. Analysis of postcapillary pH changes in blood in vivo after gas exchange. *J. Appl. Physiol.* 44: 770–781, 1978.
11. BIDANI, A., S. J. MATHEW, AND E. D. CRANDALL. Pulmonary vascular carbonic anhydrase activity. *J. Appl. Physiol.* 55: 75–83, 1983.
12. BISOGNANO, J. D., J. A. DIX, P. R. PRATAP, T. S. NOVAK, AND J. C. FREEDMAN. Proton (or hydroxide) fluxes and the biphasic osmotic response of human red blood cells. *J. Gen. Physiol.* 102: 99–123, 1993.
13. BÖNING, D., H. J. SCHÜNEMANN, N. MAASSEN, AND M. W. BUSSE. Reduction of oxylabile CO_2 in human blood by lactate. *J. Appl. Physiol.* 74: 710–714, 1993.
14. BOOTH, V. H. The carbonic anhydrase inhibitor in serum. *J. Physiol. (Lond.)* 91: 474–489, 1938.
15. BORON, W. F., S. J. WAISBREN, I. M. MODLIN, AND J. P. GEIBEL. Unique permeability barrier of the apical surface of parietal and chief cells in isolated perfused gastric glands. *J. Exp. Biol.* 196: 347–360, 1994.
16. BRAHM, J. Temperature-dependent changes of chloride transport kinetics in human red cells. *J. Gen. Physiol.* 70: 283–306, 1977.
17. BRUNS, W., R. DERMIETZEL, AND G. GROS. Carbonic anhydrase in the sarcoplasmic reticulum of the rabbit skeletal muscle. *J. Physiol. (Lond.)* 371: 351–364, 1986.
18. CARTER, N. D., AND J. AUTON. Characterisation of carbonic anhydrases from tissues of the cat. *Biochim. Biophys. Acta* 410: 220–228, 1975.
19. CHOW, E. I. H., E. D. CRANDALL, AND R. E. FORSTER. Kinetics of bicarbonate-chloride exchange across the human red blood cell membrane. *J. Gen. Physiol.* 68: 633, 1976.
20. CONLEY, K. E., S. R. KAYAR, K. RÖSLER, H. HOPPELER, E. R. WEIBEL, AND C. R. TAYLOR. Adaptive variation in the mammalian respiratory system in relation to energetic demand. IV. Capillaries and their relationship to oxidative capacity. *Respir. Physiol.* 69: 47–64, 1987.
21. CÔTÉ, C. H., N. JOMPHE, A. ODEIMAT, AND P. FRÉMONT. Carbonic anhydrase in mouse skeletal muscle and its influence on contractility. *Biochem. Cell. Biol.* 72: 244–249, 1994.
22. CRANDALL, E. D., R. A. KLOCKE, AND R. E. FORSTER. Hydroxyl ion movements across the human erythrocyte membrane. *J. Gen. Physiol.* 57: 664–683, 1971.
23. CRANDALL, E. D., S. J. MATHEW, R. S. FLEISCHER, H. I. WINTER, AND A. BIDANI. Effects of inhibition of RBC HCO_3^-/Cl^- exchange on CO_2 excretion and downstream pH disequilibrium in isolated rat lungs. *J. Clin. Invest.* 68: 853–862, 1981.
24. DECKER, B., S. SENDER, AND G. GROS. Membrane-associated carbonic anhydrase IV in skeletal muscle: subcellular localization. *Histochem. Cell. Biol.* 106: 405–411, 1996.
25. DEHEMPTINNE, A., R. MARANNES, AND B. VANHEEL. Surface pH and the control of intracellular pH in cardiac and skeletal muscle. *Can. J. Physiol. Pharmacol.* 65: 970–977, 1987.
26. DERMIETZEL, R., A. LEIBSTEIN, W. SIFFERT, N. ZAMBOGLOU, AND G. GROS. A fast screening method for histochemical localization of carbonic anhydrase. *J. Histochem. Cytochem.* 33: 93–98, 1985.
27. DEUTICKE, B., E. BEYER, AND B. FORST. Discrimination of three parallel pathways of lactate transport in the human erythrocyte membrane by inhibitors and kinetic properties. *Biochim. Biophys. Acta* 684: 96–110, 1982.
28. DIMBERG, K., L. B. HÖGLUND, P. G. KNUTSSON, AND Y. RIDDERSTRALE. Histochemical localization of carbonic anhydrase in gill lamellae from young salmon (*Salmo salar L.*) adapted to fresh and salt water. *Acta Physiol. Scand.* 112: 218–220, 1981.
29. DODGSON, S. J., AND L. C. CONTINO. Rat kidney mitochondrial carbonic anhydrase. *Arch. Biochem. Biophys.* 260: 334–341, 1988.
30. DODGSON, S. J., AND R. E. FORSTER. Carbonic anhydrase activity of intact erythrocytes from seven mammals. *J. Appl. Physiol.* 55: 1292–1298, 1983.
31. DODGSON, S. J., AND R. E. FORSTER. Inhibition of CA V decreases glucose synthesis from pyruvate. *Arch. Biochem. Biophys.* 251: 198–204, 1986.
32. DODGSON, S. J., AND R. E. FORSTER. Carbonic anhydrase: inhibition results in decreased urea production by hepatocytes. *J. Appl. Physiol.* 60: 646–652, 1986.
33. DODGSON, S. J., R. E. FORSTER, W. S. SLY, AND R. E. TASHIAN. Carbonic anhydrase activity of intact carbonic anhydrase II-deficient human erythrocytes. *J. Appl. Physiol.* 65: 1472–1480, 1988.
34. DODGSON, S. J., R. E. FORSTER, B. T. STOREY, AND L. MELA. Mitochondrial carbonic anhydrase. *Proc. Natl. Acad. Sci. USA* 77: 5562–5566, 1980.
35. EDSALL, J. T. Carbon dioxide, carbonic acid and bicarbonate ion: physical properties and kinetics of interconversion. In: *CO_2: Chemical, Biochemical and Physiological Aspects*, edited by R. E. Forster, J. T. Edsall, A. B. Otis, and F. J. W. Roughton. Washington, DC: NASA, 1969, p. SP-188.
36. EFFROS, R. M., R. S. Y. CHANG, AND P. SILVERMAN. Acceleration of plasma bicarbonate conversion to carbon dioxide by pulmonary carbonic anhydrase. *Science* 199: 427–429, 1978.
37. EFFROS, R. M., K. TAKI, P. DODEK, J. EDWARDS, A. HUSCZUK, P. SILVERMAN, AND J. HUKKANEN. Exchange of labeled bicarbonate and carbon dioxide with erythrocytes suspended in an elutriator. *J. Appl. Physiol.* 64: 569–576, 1988.
38. EFFROS, R. M., AND M. L. WEISSMAN. Carbonic anhydrase activity of the cat hind leg. *J. Appl. Physiol.* 47: 1090–1098, 1979.
39. ELLORY, J. C., M. W. WOLOWYK, AND J. D. YOUNG. Hagfish (*Eptatretus stouti*) erythrocytes show minimal chloride transport. *J. Exp. Biol.* 129: 377–383, 1987.
40. ENNS, T. Facilitation by carbonic anhydrase of carbon dioxide transport. *Science* 155: 44–47, 1967.
41. FARMER, R. E. L., AND R. I. MACEY. Pertubation of red cell volume: rectification of osmotic flow. *Biochim. Biophys. Acta* 196: 53–65, 1970.
42. FISHBEIN, W. N., J. I. DAVIS, J. W. FOELLMER, AND M. R. CASEY. Clinical assay of the human erythrocyte lactate transporter. Analysis and display of normal human data. *Biochem. Med. Metab. Biol.* 39: 351–359, 1988.
43. FORSTER, R. E. Rate of reaction of CO_2 with human hemoglobin. In: *CO_2: Chemical, Biochemical, and Physiological Aspects*, edited by R. E. Forster, J. T. Edsall, A. B. Otis, and F. J. W. Roughton. Washington, DC: NASA, 1969, p. SP-188.
44. FORSTER, R. E., H. P. CONSTANTINE, M. R. CRAW, H. H. ROTMAN, AND R. A. KLOCKE. Reaction of CO_2 with human hemoglobin solution. *J. Biol. Chem.* 243: 3317–3326, 1968.
45. FORSTER, R. E., AND E. D. CRANDALL. Time course of exchanges between red cells and extracellular fluid during CO_2 uptake. *J. Appl. Physiol.* 38: 710–718, 1975.
46. FORSTER, R. E., AND N. ITADA. Carbonic anhydrase activity in intact red cells as measured by means of ^{18}O exchange between CO_2 and water. In: *Biophysics and Physiology of Carbon Dioxide*,

edited by C. Bauer, G. Gros, and H. Bartels. Heidelberg, Germany: Springer-Verlag, 1980.
47. FORSTER, R. E., G. GROS, L. LIN, Y. ONO, AND M. WUNDER. The effect of 4,4′-diisothiocyanato-stilbene-2,2′-disulfonate on CO_2 permeability of the red blood cell membrane. *Proc. Natl. Acad. Sci. USA* 95: 15815–15820, 1998.
48. GASBJERG, P. K., AND J. BRAHM. Kinetics of bicarbonate and chloride transport in human red cell membranes. *J. Gen. Physiol.* 97: 321–349, 1991.
49. GEERS, C., O. BERTRAM, AND G. GROS. Extracellular carbonic anhydrase and blood pH equilibrium in exercising skeletal muscle (Abstract). *Pflügers Arch.* 433: P449, 1997.
50. GEERS, C., AND G. GROS. Inhibition properties and inhibition kinetics of an extracellular carbonic anhydrase in perfused skeletal muscle. *Respir. Physiol.* 56: 269–287, 1984.
51. GEERS, C., G. GROS, AND A. GÄRTNER. Extracellular carbonic anhydrase of skeletal muscle associated with the sarcolemma. *J. Appl. Physiol.* 59: 548–558, 1985.
52. GEERS, C., AND G. GROS. Carbonic anhydrase inhibition affects contraction of directly stimulated rat soleus. *Life Sci.* 42: 37–45, 1988.
53. GEERS, C., AND G. GROS. Effects of carbonic anhydrase inhibitors on contraction, intracellular pH and energy-rich phosphates of rat skeletal muscle. *J. Physiol. (Lond.)* 423: 279–297, 1990.
54. GEERS, C., D. KRÜGER, W. SIFFERT, A. SCHMID, W. BRUNS, AND G. GROS. Carbonic anhydrase in skeletal and cardiac muscle from rabbit and rat. *Biochem. J.* 282: 165–171, 1992.
55. GEERS, C., P. WETZEL, AND G. GROS. Is carbonic anhydrase required for contraction of skeletal muscle? *News Physiol. Sci.* 6: 78–82, 1991.
56. GLIBOWICKA, M., B. WINCKLER, N. ARANIBAR, M. SCHUSTER, H. HANSSUM, H. RÜTERJANS, AND H. PASSOW. Temperature dependence of anion transport in the human red blood cell. *Biochim. Biophys. Acta* 946: 345–358, 1988.
57. GRAY, B. A. The rate of approach to equilibrium in uncatalyzed CO_2 hydration reactions: the theoretical effect of buffering capacity. *Respir. Physiol.* 11: 223–234, 1971.
58. GROS, G. Mechanisms of CO_2 transport in vertebrates. *Verh. Deutsch. Zool. Ges.* 84: 213–230, 1991.
59. GROS, G., AND I. BARTAG. Permeability of the red cell membrane for CO_2 and O_2 (Abstract). *Pflügers Arch.* 382: R21, 1979.
60. GROS, G., AND S. J. DODGSON. Velocity of CO_2 exchange in muscle and liver. *Annu. Rev. Physiol.* 50: 669–694, 1988.
61. GROS, G., R. E. FORSTER, AND L. LIN. The carbamate reaction of glycylglycine, plasma, and tissue extracts evaluated by a pH stopped flow apparatus. *J. Biol. Chem.* 251: 4398–4407, 1976.
62. GROS, G., H. GROS, AND D. LAVALETTE. Facilitated proton transfer in protein solutions by rotational and translational proton diffusion. In: *Biophysics of Water*, edited by F. Franks and S. F. Mathias. Chichester, UK: Wiley, 1982, p. 225–230.
63. GROS, G., D. LAVALETTE, W. MOLL, H. GROS, B. AMAND, AND F. POCHON. Evidence for rotational contribution to protein-facilitated proton transport. *Proc. Natl. Acad. Sci. USA* 81: 1710–1714, 1984.
64. GROS, G., AND W. MOLL. The diffusion of carbon dioxide in erythrocytes and hemoglobin solutions. *Pflügers Arch.* 324: 249–266, 1971.
65. GROS, G., AND W. MOLL. The facilitated diffusion of CO_2 in hemoglobin solution and phosphate solution. In: *Oxygen Affinity of Hemoglobin and Red Cell Acid Base Status*, edited by M. Rørth and P. Astrup. New York: Academic, 1972.
66. GROS, G., AND W. MOLL. Facilitated diffusion of CO_2 across albumin solutions. *J. Gen. Physiol.* 64: 356–371, 1974.
67. GROS, G., W. MOLL, H. HOPPE, AND H. GROS. Proton transport by phosphate diffusion: a mechanism of facilitated CO_2 transfer. *J. Gen. Physiol.* 67: 773–790, 1976.
68. GROS, G., H. S. ROLLEMA, AND R. E. FORSTER. The carbamate equilibrium of α- and ϵ-amino groups of human hemoglobin at 37°C. *J. Biol. Chem.* 256: 5471–5480, 1981.
69. GROS, G., B. WITTMANN, AND L. GUGGENBERGER. Carbamate kinetics of blood proteins. *Prog. Respir. Res.* 16: 205–210, 1981.
70. GROSSIE, J., C. COLLINS, AND M. JULIAN. Bicarbonate and fast-twitch muscle: evidence for a major role in pH regulation. *J. Membr. Biol.* 105: 265–272, 1988.
71. GUTKNECHT, J., M. A. BISSON, AND F. C. TOSTESON. Diffusion of carbon dioxide through lipid bilayer membranes: effect of carbonic anhydrase, bicarbonate, and unstirred layers. *J. Gen. Physiol.* 69: 779–794, 1977.
72. HARALDSSON, B., AND B. RIPPE. Restricted diffusion of CrEDTA and cyanocobalamine across the exchange vessels in rat hindquarters. *Acta Physiol. Scand.* 127: 359–372, 1986.
73. HARTLING, O. J., H. KELBÆK, T. GJØRUP, B. SCHIBYE, K. KLAUSEN, AND J. TRAP-JENSEN. Forearm oxygen uptake during maximal forearm dynamic exercise. *Eur. J. Appl. Physiol.* 58: 466–470, 1989.
74. HASWELL, M. S., J. P. RAFFIN, AND C. LERAY. An investigation of the carbonic anhydrase inhibitor in eel plasma. *Comp. Biochem. Physiol. A Physiol.* 74: 175–177, 1983.
75. HASWELL, M. S., AND D. J. RANDALL. Carbonic anhydrase inhibitor in trout plasma. *Respir. Physiol.* 28: 17–27, 1976.
76. HEMING, T. A., C. GEERS, G. GROS, A. BIDANI, AND E. D. CRANDALL. Effects of dextran-bound inhibitors on carbonic anhydrase activity in isolated rat lungs. *J. Appl. Physiol.* 61: 1849–1856, 1986.
77. HEMING, T. A., AND D. J. RANDALL. Fish erythrocytes are bicarbonate permeable: problems with determining carbonic anhydrase activity using the modified boat technique. *J. Exp. Zool.* 219: 125–128, 1982.
78. HEMING, T. A., C. G. VANOYE, E. K. STABENAU, E. D. ROUSH, C. A. FIERKE, AND A. BIDANI. Inhibitor sensitivity of pulmonary vascular carbonic anhydrase. *J. Appl. Physiol.* 75: 1642–1649, 1993.
79. HENRY, R. P. Multiple roles of carbonic anhydrase in cellular transport and metabolism. *Annu. Rev. Physiol.* 58: 523–538, 1996.
80. HENRY, R. P., R. G. BOUTILIER, AND B. L. TUFTS. Effects of carbonic anhydrase inhibition on the acid base status in lamprey and trout. *Respir. Physiol.* 99: 241–248, 1995.
81. HENRY, R. P., B. L. TUFTS, AND R. G. BOUTILIER. The distribution of carbonic anhydrase type I and II isozymes in lamprey and trout: possible coevolution with erythrocyte chloride/bicarbonate exchange. *J. Comp. Physiol. B Biochem. Syst. Environ. Physiol.* 163: 380–388, 1993.
82. HENRY, R. P., Y. WANG, AND C. M. WOOD. Carbonic anhydrase facilitates CO_2 and NH_3 transport across the sarcolemma of the trout white muscle. *Am. J. Physiol. Regulatory Integrative Comp. Physiol.* 272: R1754—R1761, 1997.
83. HILL, E. Inhibition of carbonic anhydrase by plasma of dogs and rabbits. *J. Appl. Physiol.* 60: 191–197, 1986.
84. HILL, E. P., G. G. POWER, AND L. D. LONGO. Mathematical simulation of pulmonary O_2 and CO_2 exchange. *Am. J. Physiol.* 224: 904–917, 1973.
85. HILPERT, P., R. G. FLEISCHMANN, D. KEMPE, AND H. BARTELS. The Bohr effect related to blood and erythrocyte pH. *Am. J. Physiol.* 205: 337–340, 1963.
86. HONIG, C. R., M. L. FELDSTEIN, AND J. L. FRIERSON. Capillary lengths, anastomoses, and estimated capillary transit times in skeletal muscle. *Am. J. Physiol. Heart Circ. Physiol.* 233: H122—H129, 1977.
87. HOPPELER, H., AND R. BILLETER. Conditions for oxygen and substrate transport in muscles in exercising mammals. *J. Exp. Biol.* 160: 263–283, 1991.
88. ITADA, N., AND R. E. FORSTER. Carbonic anhydrase activity in intact red blood cells measured with ^{18}O exchange. *J. Biol. Chem.* 252: 3851–3890, 1977.
89. JACOBS, M. H., AND D. R. STEWART. The role of carbonic anhydrase in certain ionic exchanges involving the erythrocyte. *J. Gen. Physiol.* 25: 539–552, 1942.
90. JENNINGS, M. L. Structure and function of the red blood cell anion transport protein. *Annu. Rev. Biophys. Biophys. Chem.* 18: 397–430, 1989.
91. JUEL, C. Muscle lactate transport studied in sarcolemmal giant vesicles. *Biochim. Biophys. Acta* 1065: 15–20, 1991.
92. JUEL, C. Regulation of cellular pH in skeletal muscle fiber types, studied with sarcolemmal giant vesicles obtained from rat muscles. *Biochim. Biophys. Acta* 1265: 127–132, 1995.
93. JUEL, C. Symmetry and pH dependency of the lactate/proton car-

rier in skeletal muscle studied with rat sarcolemmal giant vesicles. *Biochim. Biophys. Acta* 1283: 106–110, 1996.
94. JUEL, C. Lactate-proton cotransport in skeletal muscle. *Physiol. Rev.* 77: 321–358, 1997.
95. JUEL, C., J. BANGSBO, T. GRAHAM, AND B. SALTIN. Lactate and potassium fluxes from human skeletal muscle during and after intense, dynamic, knee extensor exercise. *Acta Physiol. Scand.* 140: 147–159, 1990.
96. KANAANI, J., AND H. GINSBURG. Transport of lactate in *Plasmodium falciparum*-infected human erythrocytes. *J. Cell. Physiol.* 149: 469–476, 1991.
97. KAWASHIRO, T., AND P. SCHEID. Measurement of Krogh's diffusion constant of CO_2 in respiring muscle at various CO_2 levels: evidence for facilitated diffusion. *Pflügers Arch.* 362: 127–133, 1976.
98. KAYAR, S. R., H. HOPPELER, J. H. JONES, K. LONGWORTH, R. B. ARMSTRONG, M. H. LAUGHLIN, S. L. LINDSTEDT, J. E. P. W. BICUDO, K. GROEBE, C. R. TAYLOR, AND E. R. WEIBEL. Capillary blood transit time in muscles in relation to body size and aerobic capacity. *J. Exp. Biol.* 194: 69–81, 1994.
99. KHALIFAH, R. G. The carbon dioxide hydration activity of carbonic anyhdrase. *J. Biol. Chem.* 246: 2561–2573, 1971.
100. KIFOR, G., M. R. TOON, A. JANOSHAZI, AND A. K. SOLOMON. Interaction between red cell membrane band 3 and cytosolic carbonic anhydrase. *J. Membr. Biol.* 134: 169–179, 1993.
101. KILMARTIN, J. V. Influence of DPG on the Bohr effect of human hemoglobin. *FEBS Lett.* 38: 147–148, 1974.
102. KLOCKE, R. A. Mechanism and kinetics of the Haldane effect in human erythrocytes. *J. Appl. Physiol.* 35: 673–681, 1973.
103. KLOCKE, R. A. Rate of bicarbonate-chloride exchange in human red cells at 37°C. *J. Appl. Physiol.* 40: 673–681, 1973.
104. KLOCKE, R. A. Catalysis of CO_2 reactions by lung carbonic anhydrase. *J. Appl. Physiol.* 44: 882–888, 1978.
105. KLOCKE, R. A. Carbon dioxide transport. In: *Handbook of Physiology. The Respiratory System. Gas Exchange.* Bethesda, MD: Am. Physiol. Soc., 1987, sect. 3, vol. IV, chapt. 10, p. 173–198.
106. KOWALCHUK, J. M., G. J. F. HEIGENHAUSER, J. R. SUTTON, AND N. L. JONES. Effect of acetazolamide on gas exchange and acid-base control after maximal exercise. *J. Appl. Physiol.* 72: 278–287, 1992.
107. KUSHMERICK, M. J., AND R. J. PODOLSKY. Ionic mobility in muscle cells. *Science* 166: 1297–1298, 1969.
108. LANDOLT, H., AND R. BÖRNSTEIN. *Zahlenwerte und Funktionen.* Berlin: Springer, 1960.
109. LEINER, M., H. BECK, AND H. ECKERT. Über die Kohlensäure-Dehydratase in den einzelnen Wirbeltierklassen. *Hoppe-Seyler's Z. Physiol. Chem.* 327: 144–165, 1962.
110. LINDINGER, M. I., R. S. MCKELVIE, AND G. J. F. HEIGENHAUSER. K^+ and Lac^+ distribution in humans during and after high-intensity exercise: role in muscle fatigue attenuation? *J. Appl. Physiol.* 78: 765–777, 1995.
111. LONGMUIR, I. S., R. E. FORSTER, AND C. Y. WOO. Diffusion of carbon dioxide through thin layers of solution. *Nature* 209: 393–394, 1966.
112. MACLEAN, D. A., B. SALTIN, AND J. BANGSBO. Interstitial muscle glucose and lactate levels during dynamic exercise in humans determined by microdialysis (Abstract). *Pflügers Arch.* 430: R69, 1995.
113. MAREN, T. H. Carbonic anhydrase: chemistry, physiology and inhibition. *Physiol. Rev.* 47: 595–781, 1967.
114. MAREN, T. H., B. R. FRIEDLAND, AND R. S. RITTMASTER. Kinetic properties of primitive vertebrate carbonic anhydrases. *Comp. Biochem. Physiol. B Biochem.* 67: 69–74, 1980.
115. MAREN, T. H., AND G. SANYAL. The activity of sulfonamides and anions against the carbonic anhydrases of animals, plants and bacteria. *Annu. Rev. Pharmacol. Toxicol.* 23: 439–459, 1983.
116. MEISSNER, G. Calcium transport and monovalent cation and proton fluxes in sarcoplasmic reticulum vesicles. *J. Biol. Chem.* 256: 636–643, 1981.
117. MEISSNER, G., AND R. C. YOUNG. Proton permeability of sarcoplasmic reticulum vesicles. *J. Biol. Chem.* 255: 6814–6819, 1980.
118. MELDRUM, N. U., AND F. J. W. ROUGHTON. Carbonic anhydrase. Its preparation and properties. *J. Physiol. (Lond.)* 80: 113–142, 1933.
119. METZGER, J. M., AND R. H. FITTS. Role of intracellular pH in muscle fatigue. *J. Appl. Physiol.* 62: 1392–1397, 1987.
120. MICHEL, C. C. Capillary permeability and how it may change. *J. Physiol. (Lond.)* 404: 1–29, 1988.
121. MITHOEFER, J. C. Inhibition of carbonic anhydrase: its effect on carbon dioxide elimination by the lung. *J. Appl. Physiol.* 14: 109–115, 1959.
122. MITHOEFER, J. C., AND J. S. DAVIS. Inhibition of carbonic anhydrase: effect on tissue gas tensions in the rat. *Proc. Soc. Exp. Biol. Med.* 98: 797–801, 1958.
123. MOORE, W. J. Electrochemistry: conductance and ionic reactions. In: *Physical Chemistry.* London: Prentice-Hall, 1962.
124. NAGAO, Y., M. SRINIVASAN, J. S. PLATERO, M. SVENDROWSKI, A. WAHEED, AND W. S. SLY. Mitochondrial carbonic anhydrase (isozyme V) in mouse and rat: cDNA cloning, expression, subcellular localization, processing, and tissue distribution. *Proc. Natl. Acad. Sci. USA* 91: 10330–10334, 1994.
125. NIELSEN, S., B. L. SMITH, E. I. CHRISTENSEN, AND P. AGRE. Distribution of the aquaporin CHIP in secretory and resorptive epithelia and capillary endothelia. *Proc. Natl. Acad. Sci. USA* 90: 7275–7279, 1993.
126. NIKINMAA, M. Oxygen and carbon dioxide transport in vertebrate erythrocytes: an evolutionary change in the role of membrane transport. *J. Exp. Biol.* 200: 369–380, 1997.
127. NORRIS, F. A., AND G. L. POWELL. Characterization of CO_2/carbonic acid mediated proton flux through phosphatidylcholine vesicles as model membranes. *Biochim. Biophys. Acta* 1111: 17–26, 1992.
128. OBAID, A. L., A. M. CRITZ, AND E. D. CRANDALL. Kinetics of bicarbonate/chloride exchange in dogfish erythrocytes. *Am. J. Physiol. Regulatory Integrative Comp. Physiol.* 237: R132—R138, 1979.
129. O BRASKY, J. E., AND E. D. CRANDALL. Organ and species differences in tissue vascular carbonic anhydrase activity. *J. Appl. Physiol.* 49: 211–217, 1980.
130. OHLIGER, D. E., C. J. LYNCH, R. E. FORSTER, AND S. J. DODGSON. Amino acid sequence of rat CA V (Abstract). *FASEB J.* 7: A676, 1993.
131. OHNISHI, S. T., AND H. ASAI. Lamprey erythrocytes lack glycoproteins and anion transport. *Comp. Biochem. Physiol. B Biochem.* 81: 405–408, 1985.
132. PAPPENHEIMER, J. R. Passage of molecules through capillary wall. *Physiol. Rev.* 33: 387–423, 1953.
133. PARKES, J. L., AND P. S. COLEMAN. Enhancement of carbonic anhydrase activity by erythrocyte membranes. *Arch. Biochem. Biophys.* 275: 459–468, 1989.
134. PERELLA, M., G. GUGLIELMO, AND A. MOSCA. Determination of the equilibrium constants for oxygen-linked CO_2 binding to human hemoglobin. *FEBS Lett.* 78: 287–290, 1977.
135. PERELLA, M., J. V. KILMARTIN, F. FOGG, AND L. ROSSI-BERNARDI. Identification of the high and low affinity CO_2-binding sites of human haemoglobin. *Nature* 256: 759–761, 1975.
136. PETERS, T., AND G. GROS. Transport of bicarbonate, other ions and substrates across the red blood cell membrane of hagfishes. In: *The Biology of Hagfishes*, edited by J. M. Jørgensen, J. P. Lomholt, R. E. Weber, and H. Malte. London: Chapman & Hall, 1998.
137. PETERS, T., F. STASCHEN, H. P. KUBIS, AND G. GROS. Carbonic anhydrase inhibitor in the plasma of the flounder (*Platichtys flesus*). *Pflügers Arch.* 429: R127, 1995.
138. POOLE, R. C., AND A. P. HALESTRAP. Transport of lactate and other monocarboxylates across mammalian plasma membranes. *Am. J. Physiol. Cell Physiol.* 264: C761—C782, 1993.
139. RANDALL, R. F., AND T. H. MAREN. Absence of carbonic anhydrase in red cell membranes. *Biochim. Biophys. Acta* 268: 730–732, 1972.
140. RIDDERSTRALE, Y. Observations on the localization of carbonic anhydrase in muscle. *Acta Physiol. Scand.* 106: 239–240, 1979.
141. RILEY, D. A., S. ELLIS, AND J. BAIN. Carbonic anhydrase activity in skeletal muscle fiber types, axons, spindles and capillaries of rat soleus and extensor digitorum longus muscles. *J. Histochem. Cytochem.* 30: 1275–1288, 1982.
142. RISPENS, P., C. W. DELLEBARRE, D. ELEVELD, W. HELDER, AND W. G. ZIJLSTRA. The apparent first dissociation constant of car-

bonic acid in plasma between 16 and 42.5°C. *Clin. Chim. Acta* 22: 627–637, 1968.
143. ROMANOWSKI, F., J. SCHIERENBECK, AND G. GROS. Facilitated CO_2 diffusion in various striated muscles. In: *Quantitative Spectroscopy in Tissue*, edited by K. Frank and M. Kessler. Frankfurt, Germany: PMI-Verlag, 1992.
144. ROOS, A., AND W. F. BORON. Intracellular pH transients in rat diaphragm muscle measured with DMO. *Am. J. Physiol. Cell Physiol.* 235: C49—C54, 1978.
145. ROSENBERG, S. A., AND G. GUIDOTTI. The protein of human erythrocyte membranes. *J. Biol. Chem.* 243: 1985–1992, 1968.
146. ROUGHTON, F. J. W. Recent work on carbon dioxide transport by the blood. *Physiol. Rev.* 15: 241–296, 1935.
147. ROUGHTON, F. J. W. Transport of oxygen and carbon dioxide. In: *Handbook of Physiology. Respiration.* Washington, DC: Am. Physiol. Soc., 1964, sect. 3, vol. I, chapt. , p. .
148. ROUGHTON, F. J. W., D. B. DILL, R. C. DARLIN, A. GRAYBIEL, C. A. KNEHR, AND J. H. TALBOTT. Some effects of sulfanilamide on man at rest and during exercise. *Am. J. Physiol.* 135: 77–87, 1941.
149. ROUSH, E. D., AND C. A. FIERKE. Purification and characterization of a carbonic anhydrase II inhibitor from porcine plasma. *Biochemistry* 31: 12536–12542, 1992.
150. RYAN, U. S., P. L. WHITNEY, AND J. W. RYAN. Localization of carbonic anhydrase on pulmonary artery endothelial cells in culture. *J. Appl. Physiol.* 53: 914–919, 1982.
151. SAARIKOSKI, J. M., AND K. KAILA. Simultaneous measurement of intracellular and extracellular carbonic anhydrase activity in intact muscle fibres. *Pflügers Arch.* 421: 357–363, 1992.
152. SAHLIN, K., A. ALVESTRAND, R. BRANDT, AND E. HULTMAN. Intracellular pH and bicarbonate concentration in human muscle during recovery from exercise. *J. Appl. Physiol.* 45: 474–480, 1978.
153. SALTIN, B. Hemodynamic adaptations to exercise. *Am. J. Cardiol.* 55: 42D—47D, 1985.
154. SARELIUS, I. H. Cell flow path influences transit time through striated muscle capillaries. *Am. J. Physiol. Heart Circ. Physiol.* 250: H899—H907, 1986.
155. SCHEID, P., AND W. SIFFERT. Effects of inhibiting carbonic anhydrase on isometric contraction of frog skeletal muscle. *J. Physiol. (Lond.)* 361: 91–101, 1985.
156. SENDER, S., B. DECKER, C. D. FENSKE, W. S. SLY, N. D. CARTER, AND G. GROS. Localization of carbonic anhydrase IV in rat and human heart muscle. *J. Histochem. Cytochem.* 46: 855–861, 1998.
157. SENDER, S., G. GROS, A. WAHEED, G. S. HAGEMAN, AND W. S. SLY. Immunohistochemical localization of carbonic anhdrase IV in capillaries of rat and human skeletal muscle. *J. Histochem. Cytochem.* 42: 1229–1236, 1994.
158. SEXTON, W. L., D. C. POOLE, AND O. MATHIEU-COSTELLO. Microcirculatory structure-function relationships in skeletal muscle of diabetic rats. *Am. J. Physiol. Heart Circ. Physiol.* 266: H1502—H1511, 1994.
159. SHIBATA, M., AND A. KAMIYA. Blood flow dependence of local capillary permeability of Cr-EDTA in the rabbit skeletal muscle. *Jpn. J. Physiol.* 42: 631–639, 1992.
160. SIEGER, U., J. BRAHM, AND R. BAUMANN. Chloride and bicarbonate transport in chick embryonic red blood cells. *J. Physiol. (Lond.)* 477: 393–401, 1994.
161. SIFFERT, W., AND G. GROS. Carbonic anhydrase C in white skeletal muscle tissue. *Biochem. J.* 205: 559–566, 1982.
162. SLY, W. S., AND P. Y. HU. Human carbonic anhydrases and carbonic anhydrase deficiencies. *Annu. Rev. Biochem.* 64: 375–401, 1995.
163. SLY, W. S., S. SATO, AND X. L. ZHU. Evaluation of carbonic anhydrase isozymes in disorders involving osteopetrosis and/or renal tubular acidosis. *Clin. Biochem.* 24: 311–318, 1991.
164. SOMLYO, A. V., H. GONZALES-SERRATOS, H. SHUMAN, G. MCCLELLAN, AND A. P. SOMLYO. Calcium release and ionic changes in the sarcoplasmic reticulum of tetanized muscle: an electron-probe study. *J. Cell Biol.* 90: 577–594, 1981.
165. STOREY, B. T., L. C. LIN, B. TOMPKINS, AND R. E. FORSTER. Carbonic anhydrase in guinea pig skeletal muscle mitochondria. *Arch. Biochem. Biophys.* 270: 144–152, 1989.
166. SWENSON, E. R., AND T. H. MAREN. A quantitative analysis of CO_2 transport at rest and during maximal exercise. *Respir. Physiol.* 35: 129–159, 1978.
167. SWENSON, E. R., AND T. H. MAREN. Roles of gill and red cell carbonic anhydrase in elasmobranch HCO_3^- and CO_2 excretion. *Am. J. Physiol. Regulatory Integrative Comp. Physiol.* 253: R450—R458, 1987.
168. SYME, P. D., J. K. ARONSON, C. H. THOMPSON, E. M. WILLIAMS, Y. GREEN, AND G. K. RADDA. Na^+/H^+ and HCO_3^-/Cl^- exchange in the control of intracellular pH in vivo in the spontaneously hypertensive rat. *Clin. Sci.* 81: 743–750, 1991.
169. TAKI, K., K. HIRAHARA, T. TOTOKI, AND N. TAKAHASHI. Retention of carbon dioxide in tissue following carbonic anhydrase inhibition in dogs. *Clin. Ther.* 15: 884–889, 1993.
170. TAPPAN, D. V. Carbonic anhydrase activity of erythrocyte ghosts. *Experientia* 24: 127, 1968.
171. TUFTS, B. L., AND R. G. BOUTILIER. The absence of rapid chloride/bicarbonate exchange in lamprey erythrocytes: implications for CO_2 transport and ion distributions between plasma and erythrocytes in the blood of *Petromyzon marinus*. *J. Exp. Biol.* 144: 565–576, 1989.
172. TUFTS, B. L., AND R. G. BOUTILIER. CO_2 transport properties of the blood of a primitive vertebrate, *Myxine glutinosa* (L.). *Exp. Biol.* 48: 341–347, 1990.
173. UCHIDA, K., M. MOCHIZUKI, AND K. NIIZEKI. Diffusion coefficients of CO_2 molecule and bicarbonate ion in hemoglobin solution measured by fluorescence technique. *Jpn. J. Physiol.* 33: 619–634, 1983.
174. VÄÄNÄÄNEN, H. K., N. D. CARTER, AND S. J. DODGSON. Immunocytochemical localization of mitochondrial carbonic anhydrase in rat tissues. *J. Histochem. Cytochem.* 39: 451–459, 1991.
175. WAHEED, A., X. L. ZHU, W. S. SLY, P. WETZEL, AND G. GROS. Rat skeletal muscle membrane associated carbonic anhydrase is 39-kDa, glycosylated, GPI-anchored CA IV. *Arch. Biochem. Biophys.* 294: 550–556, 1992.
176. WAISBREN, S. J., J. P. GEIBEL, I. M. MODLIN, AND W. F. BORON. Unusual permeability properties of gastric gland cells. *Nature* 368: 332–335, 1994.
177. WATSON, P. D. Permeability of cat skeletal muscle capillaries to small solutes. *Am. J. Physiol. Heart Circ. Physiol.* 268: H184—H193, 1995.
178. WESTERBLAD, H., AND D. G. ALLEN. Changes of intracellular pH due to repetitive stimulation of single fibres from mouse skeletal muscle. *J. Physiol. (Lond.)* 449: 49–71, 1992.
179. WETZEL, P., AND G. GROS. Sarcolemmal carbonic anhydrase in red and white rabbit skeletal muscle. *Arch. Biochem. Biophys.* 279: 345–354, 1990.
180. WETZEL, P., AND G. GROS. Inhibition and kinetic properties of membrane-bound carbonic anhydrases in rabbit skeletal muscles. *Arch. Biochem. Biophys.* 356: 151–158, 1998.
181. WETZEL, P., T. LIEBNER, AND G. GROS. Carbonic anhydrase inhibition and calcium transients in soleus fibers. *FEBS Lett.* 267: 66–70, 1990.
182. WIETH, J. O., AND J. BRAHM. Cellular anion transport. In: *The Kidney: Physiology and Pathophysiology*, edited by D. W. Seldin and G. Giebisch. New York: Raven, 1985.
183. WILSON, J. R., K. K. MCCULLY, D. M. MANCINI, B. BODEN, AND B. CHANCE. Relationship of muscular fatigue to pH and diprotonated P_i in humans: a ^{31}P-NMR study. *J. Appl. Physiol.* 64: 2333–2339, 1988.
184. WISTRAND, P. J. The importance of carbonic anhydrase B and C for the unloading of CO_2 by the human erythrocyte. *Acta Physiol. Scand.* 113: 417–426, 1981.
185. WITTENBERG, B. A., AND J. B. WITTENBERG. Transport of oxygen in muscle. *Annu. Rev. Physiol.* 51: 857–878, 1989.
186. WOOD, C. M., AND R. S. MUNGER. Carbonic anhydrase injection provides evidence for the role of blood acid-base status in stimulating ventilation after exhaustive exercise in rainbow trout. *J. Exp. Biol.* 194: 225–253, 1994.
187. WOOD, C. M., S. F. PERRY, P. J. WALSH, AND S. THOMAS. HCO_3^- dehydration by the blood of an elasmobranch in the absence of a Haldane effect. *Respir. Physiol.* 98: 319–337, 1994.
188. WOODBURY, J. W., AND P. R. MILES. Anion conductance of frog muscle membranes: one channel, two kinds of pH dependence. *J. Gen. Physiol.* 62: 324–353, 1973.
189. ZBOROWSKA-SLUIS, D. T., A. L. L'ABBATE, AND G. A. KLASEN. Evidence of carbonic anhydrase activity in skeletal muscle: a role for facilitative carbon dioxide transport. *Respir. Physiol.* 21: 341–350, 1974.